DESIGN AND ANALYSIS OF ANTENNAS MOUNTED ON CYLINDERS FOR AVIONICS APPLICATIONS

A THESIS SUBMITTED TO
THE GRADUATE SCHOOL OF NATURAL AND APPLIED SCIENCES
OF
MIDDLE EAST TECHNICAL UNIVERSITY

BY

MUSTAFA ÖZCAN

IN PARTIAL FULFILLMENT OF THE REQUIREMENTS
FOR
THE DEGREE OF MASTER OF SCIENCE
IN
ELECTRIC AND ELECTRONICS ENGINEERING

JULY 2015

Approval of the thesis:

DESIGN AND ANALYSIS OF ANTENNAS MOUNTED ON CYLINDERS FOR AVIONICS APPLICATIONS

submitted by **MUSTAFA ÖZCAN**in partial fulfillment of the requirements for the degree of **Master of Science in Electrical And Electronics Engineering Department, Middle East Technical University** by,

Prof. Dr. Gülbin Dural Ünver _____
Dean, Graduate School of **Natural and Applied Sciences**

Prof. Dr. Gönül Turhan Sayan _____
Head of Department, **Electrical and Electronics Eng.**

Prof. Dr. Özlem Aydın Çivi _____
Supervisor, **Electrical and Electronics Eng. Dept., METU**

Examining Committee Members:

Prof. Dr. Sencer Koç _____
Electric and Electronics Eng. Dept., METU

Prof. Dr. Özlem Aydın Çivi _____
Electric and Electronics Eng. Dept., METU

Prof. Dr. Birsen Saka _____
Electric and Electronics Eng. Dept., Hacettepe University

Assoc. Dr. Lale Alatan _____
Electric and Electronics Eng. Dept., METU

Prof. Dr. Gülbin Dural Ünver _____
Electric and Electronics Eng. Dept., METU

Date: 09.07.2015

I hereby declare that all information in this document has been obtained and presented in accordance with academic rules and ethical conduct. I also declare that, as required by these rules and conduct, I have fully cited and referenced all material and results that are not original to this work.

Name, Last Name : Mustafa ÖZCAN

Signature :

ABSTRACT

DESIGN AND ANALYSIS OF ANTENNAS MOUNTED ON CYLINDERS FOR AVIONICS APPLICATIONS

Özcan, Mustafa
M.S., Department of Electrical and Electronics Engineering
Supervisor: Prof. Dr. Özlem Aydın Çivi

July 2015, 78 pages

Conformal antenna structures are widely used in airframes because of not disturbing the aerodynamic characteristics. In this study, stripline fed conformal slot antennas of rectangular and rounded bow-tie shaped geometries, and coplanar patch antennas are designed to comply with the design requirements of a telemetry application in the frequency band of 2225-2275 MHz. Furthermore, parametric studies are carried out for some crucial design parameters in order to understand the relation between the antenna physical dimensions and electromagnetic behavior such as S_{11}, bandwidth and far-field patterns. All designed antennas are fabricated and measured to validate the simulation results. Although there are some problems occurred during fabrication process, measurement and simulation results agree well with each other. It is demonstrated that operating bandwidth of developed rounded bow-tie shaped slot antenna is 2225-2275 MHz.

KEYWORDS : Stripline fed slot antenna, Coplanar patch antenna, S_{11}-parameter, Parametric simulation

ÖZ

AVİYONİK UYGULAMALARI İÇİN SİLİNDİR ÜSTÜNE YERLEŞTİRİLEN ANTENLERİN TASARIMI VE ANALİZİ

Özcan, Mustafa
Yüksek Lisans, Elektrik ve Elektronik Mühendisliği Bölümü
Tez Yöneticisi: Prof. Dr. Özlem Aydın Çivi

Temmuz 2015, 78 sayfa

Konformal antenler aerodinamik karakteristiklerini bozmadıklarından dolayı uçak gövdelerinde sıklıkla kullanılmaktadır. Bu çalışmada, 2225-2275 MHz frekans bandındaki bir telemetri uygulamasının tasarım gereksinimleri ile uyumlu dikdörtgensel ya da bükümlü papyon geometriye sahip konformal şerit hat beslemeli yarık antenler ile eşdüzlemsel yama antenler tasarlanmış, simule edilmiş ve üretilmiştir. Bununla birlikte, antene ait fiziksel boyutlar ile antenin S_{11}, bandgenişliği ve uzak alan örüntüsü gibi elektromanyetik davranışları arasındaki ilişkiyi anlamak amacıyla bazı önemli tasarım parametreleri ile parametrik çalışmalar gerçekleştirilmiştir. Tasarlanan tüm antenler simulasyon sonuçlarının doğrulamak amacıyla üretilmiş ve ölçülmüştür. Üretim sürecinde bazı problemler yaşanmasına karşın ölçüm ve simulasyon sonuçlarının birbirleri uyumlu oldukları gözlenmiştir. Geliştirilen bükümlü papyon geometriye sahip yarık antenin çalışma bandgenişliğinin 2225-2275 MHz aralığında olduğu gösterilmiştir.

ANAHTAR KELIMELER : Şerithat beslemeli yarık anten, Eşdüzlemsel yama anten S_{11}-parametresi, Parametrik simulasyon

To Gizem

ACKNOWLEDGEMENTS

I would like to express my gratitude to my supervisor Prof. Dr. Özlem Aydın Çivi for her valuable guidance and patience throughout this study. I would also like to thank to my colleague Ozan Koroglu for his valuable comments and insight into the topic. Without his help this study could not have been finalized. Furthermore I would like to thank Erdinç Yurdakul, who have willingly shared their precious time during the fabricating the antennas.

I would also like to thank to Undersecretariat for Defense Industries (SSM) for supporting to this study within the Researcher Growth Program for Defence Industry (SAYP)

I am grateful to ROKETSAN Inc. for the financial and technical support and opportunities in case this study is completed.

I would like to indicate my appreciations to my family for their endless supports and assistances.

Although there is no way to explain my appreciation, I would like to indicate my endless gratitude to my *fairy* Gizem Arı for her limitless support and understanding during the thesis study.

TABLE OF CONTENTS

LIST OF TABLES

TABLES

LIST OF FIGURES

FIGURES

LIST OF ABBREVIATIONS

B-SFRSA	Broadband Stripline Fed Rounded Slot Antenna
CPA	Coplanar Patch Antenna
CPW	Coplanar Waveguide
CST	Computer Simulation Technology
SFSA	Stripline Fed Slot Antenna
SMA	SubMiniature version A
SFRSA	Stripline Fed Rounded Slot Antenna
U-CPA	Updated Coplanar Patch Antenna
UAV	Unmanned Air Vehicle
WCS	Working Coordinate System

CHAPTER 1

INTRODUCTION

1.1 Overview

Conformal antenna is an antenna which conforms to any surfaces over the prescribed body. In general, for most of the applications conformal antennas have cylindrical, conical, spherical shapes. Most appropriate method to fabricate conformal antennas is to use printed antenna on flexible substrate technology.

Conformal antennas designed and produced for the high speed vehicles have special requirements. Surfaces of these type of vehicles are generally made of metallic materials to endure extreme environmental conditions. In addition, these antennas must have a low profile so that they can conform perfectly to surface of these vehicles. This is crucial because any undesired protrusion from the surface can cause aerodynamical issues and additional fuel consumption. Hence, conformal antennas for these applications should be easily placed on and also compatible with the metallic surface of the vehicles.

Microstrip patch antennas are one of the most convenient candidate for the conformal antenna arrays since they have metallic ground planes and low profiles, [1-5]. However, microstrip patch antennas have some disadvantages for these applications. These antennas printed on a thin substrate so patch radiator behaves as a cavity resonator. Thus, these antennas have narrow bandwidth, typically %1-2. The antenna bandwidth increases as the substrate thickness is increased. However, power leakage taken place due to surface wave propagation in such a configuration. Although microstrip patch antennas could be easily placed over the metallic surface of the vehicles, their surrounding is inherently dielectric. Therefore, incompatibilities

between the metallic surface of the vehicle and dielectric structure of the microstrip patch antennas are occurred [6]. Microstrip line fed patch antenna have a disadvantage of distortion in the pattern due to radiation from feed line. To avoid this, aperture couple patch antenna can be used but in this case additional ground plane should be replaced at a λ/4 distance from the microstrip feed line surface. The overall antenna becomes very thick.

There is huge literature on conformal antennas. It would be pretentious to cover the complete literature on this extensive subject. Therefore, we shall focus on some conformal antenna studies similar to the ones consider in the scope of this thesis. Single element microstrip patch antenna is designed for avionics application in [7]. Then this antenna is wrapped around a toroidal body, and differences between the planar and conformal antennas are discussed based on electromagnetic simulations. Besides, designed antenna is placed over an aircraft and effects of aircraft to the antenna are also examined by electromagnetic simulations. Another attractive conformal antenna study is given in [8]. Simulation and fabrication procedures of a GPS patch antenna for a missile is deeply explained in this study. Instead of an array, a single wide microstrip patch with a special feed network is designed so that patch width of the antenna is equal to the circumference of the missile. Designed antenna is fabricated and used in a missile firing test. Some problems due to fabrication process cause high loss in the antenna. Thus, antenna is not properly operated and locked to the adequate number of satellites.

Printed-apertures or slot antennas for the conformal antennas have some benefits with respect to the microstrip patch antennas. These antennas do not suffer from the parasitic radiation due to the feedlines and, according to the aperture geometry they have wider impedance bandwidth [9]. The slot antennas are one of the best solution for the conformal applications. However, slot element radiation is bidirectional so that a reflector must be used to eliminate the backraditaion. It is shown in [6] that optimum spacing between the slot and the reflector should be nearly one-quarter free-space wavelength to obtain a unidirectional radiation. However, antenna

thickness should be small since the antenna will be integrated in an arbitrarily curved surface. In this case, reflector should be placed close to ground plane of the slot and this is resulting in a typical stripline structure. Unfortunately, parallel-plate modes take place in the stripline structure. Reducing the distance between the feedline and top/bottom ground planes in the stripline structure is increasing the parallel-plate mode excitation. Higher-order modes are prevented by choosing a relatively thin substrate, but suppression of the fundamental transverse electromagnetic (TEM) mode is extremely difficult in very thin substrate. A well-known method for TEM mode suppression is the placements of vias around the slot. These vias provide the electrical conductivity between the bottom and top ground planes. Thus, the electric field of the TEM mode will not occur since the bottom and top ground planes are held at the same potential. However, if vias are so close to the slot aperture, the resonant and broandband behavior of the slot is dramatically affected. If vias are too far from the slot aperture, power leakage happens into the TEM mode and antenna efficiency is getting worse [6].

Another alternative antenna for the conformal antenna array is coplanar patch antenna (CPA). This type of antenna consists of a patch surrounded by closely spaced ground conductor and coplanar waveguide feed structure. This antenna seems very similar with a slot loop antenna. However, performed electromagnetic simulations show that coplanar patch antenna behaves as a microstrip patch antenna instead of a slot loop antenna. Electromagnetic simulations also show that the main controller of the operating frequency is the length of the patch radiator, [10]. However, this antenna has also disadvantages of having feed line and radiating part on the same surface.

In this study, it is intended to design, fabricate and measure conformal cylindrical antennas to use in an on-board telemetry application. Telemetry can be simply defined as data acquisition from a remote location and then relaying to a user/recorder in a base location [11]. Telemetry section of a system basically consists of three main parts. First part of the telemetry is an encoder gathered the digital and

analogue data from the system or subsystem. The encoder also put these collected data in a certain frame format. In order to generate and amplify a carrier wave and modulate it with an information signal derived from the encoder, transmitter which is a second part of the telemetry is needed. Last section is composed of the conformal antenna which converts the electrical signal to electromagnetic waves.

1.2 Objectives and Organization of the Thesis

In this thesis, stripline fed slot antennas are developed for the conformal antenna array. Feed network of these antennas does not cause any undesired effects on the patterns since these antennas are fed by stripline feed. Besides, top and bottom surfaces of the antenna are made of metallic plates so that antenna can be conformed on the vehicle surface without any discontinuity. In addition, modified coplanar patch antenna is designed and fabricated to obtain wider bandwidth.

Design, fabrication and measurement results for each antenna are expressed in the corresponding chapter. Besides, parametric studies are performed for each antenna to determine the design guidelines.

The main objectives of this thesis are as follows;

- investigate appropriate antenna types for an array that can be conformed on a metallic cylinder surface
- design, fabrication and characterization of stripline fed slot antennas with enough bandwidth for telemetry application
- design and fabrication of cylindrical array of stripline fed slots
- design, fabrication and characterization of modified coplanar patch antenna to obtain a wider bandwidth

After the brief introduction of theoretical background, design of the stripline slot antenna is presented in Chapter 2. Furthermore, parametric study of this antenna is

summarized. Fabrication details are described. Finally, comparison of measurement results with simulations is given.
The slot antenna presented in Chapter 2 does not satisfy the bandwidth requirement. To enhance the bandwidth, rounded bow-tie antenna is investigated in Chapter 3. Design, fabrication and measurement results are presented.

In the Chapter 4, details of a cylindrical conformal antenna array design consisting of bow-tie elements are presented. Furthermore, radiation characteristic of planar and cylindrical arrays are discussed and compared. Cylindrical array is simulated by both transient and frequency solver of CST. Differences between these two solvers are also discussed by comparing the simulations obtained by them.

Coplanar patch antenna is designed and produced as an alternative for the stripline fed slot antennas. This antenna and related parametric study are presented in Chapter 5. Thus, results obtained from the design and fabrication studies are discussed by considering the results of the stripline fed slot antennas.

Finally, Chapter 6 presents the conclusions of the thesis and future work.

CST Microwave Studio®, full wave electromagnetic solver is used to design all antennas presented in this thesis. Details of the procedure to model and simulate a microstrip patch antenna conformed on a cylindrical surface by CST are explained in Appendix A.

CHAPTER 2

DESIGN, FABRICATION AND MEASUREMENT OF A STRIPLINE FED RECTANGULAR SHAPED SLOT ANTENNA

In this chapter, design, fabrication and measurement of stripline fed rectangular shaped slot antenna are presented. Design guidelines are formed based on the experience obtained by parametric studies and fabrication. Design of antenna and parametric studies are given in section 2.2. The designed antenna is fabricated using PCB technology in METU EEE Department. In section 2.4, measurements of the antenna are provided and compared with the simulation results.

2.1 Design Requirements of the Antenna

The ultimate aim of this study, is to design and fabricate an array antenna which is wrapped around a metallic cylinder of radius 37 mm. first array elements are presented in Chapter 2 & 3 and then array is formed and discussed in Chapter 4.
Requirements of the antenna are given in Table 1, some of the requirements which need further clarification are also explained.

Table 1 Requirements of the Antenna

Requirements	Values
Operating frequency	2.25GHz ± 25MHz
Input impedance	50 ohm
Bandwidth	50 MHz
S_{11} (Return Loss)	≤ - 10 dB
Omni-directional pattern on the roll plane	-
Reducing the environmental effects to minimum	-

In addition to the requirements given in Table 1, antenna should be fabricated on flexible material, because it is wrapped around a cylindrical body. RO3003® high frequency circuit material manufactured by Roger Corporation is chosen due to its flexibility. Dielectric constant of the substrate is 3 and 35 μm copper is deposited to both sides of the substrate [12]. Backplane of the antenna should be ground plane to separate the radiating part from transmitting and receiving circuitry. Furthermore, pattern of the antenna should be omni-directional on the roll plane of the body shown in Figure 1, to ensure the reception of the telemetry signal for all position of the antenna placed at the system.

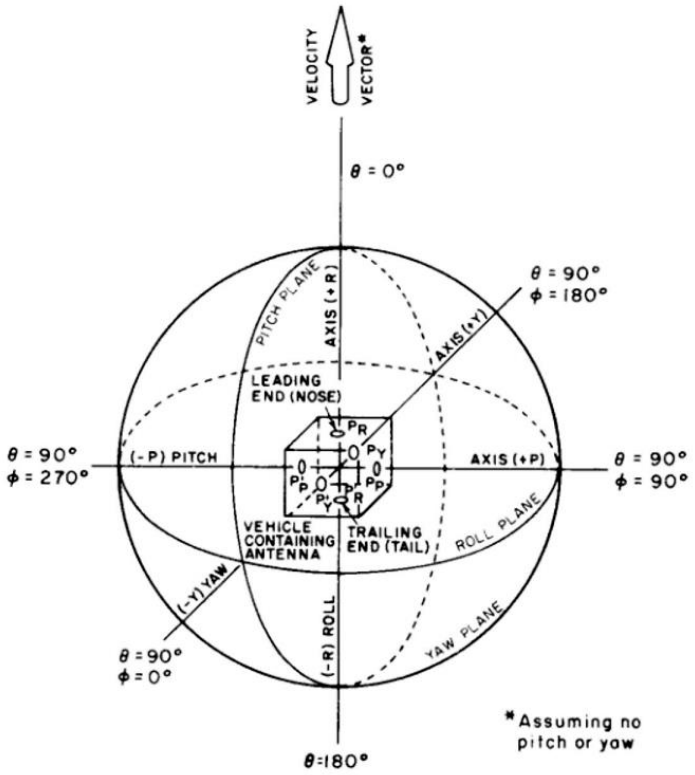

Figure 1 Coordinate System of the Antenna Placed Body [13]

2.2 Design of Stripline Fed Rectangular Shaped Slot Antenna

The structure of the stripline fed rectangular shaped slot antenna is given in Figure 2. This antenna consists of two dielectric layers. A stripline is sandwiched between these two dielectrics. Top and bottom surfaces are covered by metallic plates and a slot is etched on the upper conductor.

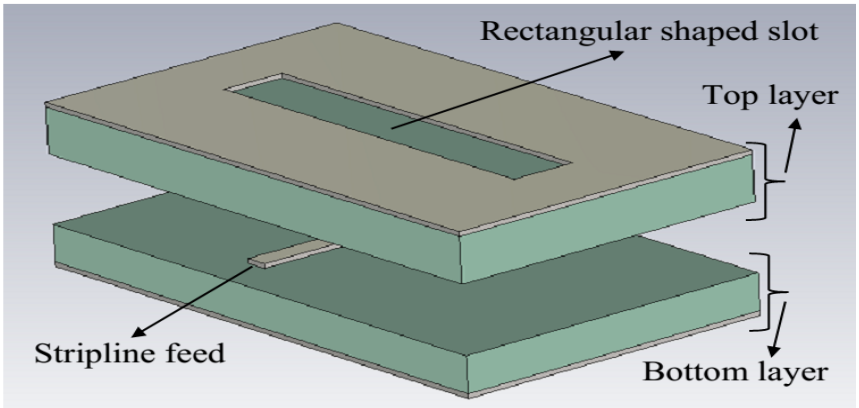

Figure 2 Stripline fed rectangular shaped slot antenna design

Operating frequency of the antenna mainly depends on the electrical length of the slot. It is well known that slot and dipole antennas are complementary structures. Thus, length of the slot can be determined by considering the complementary model of the slot antenna, [14]. Complementary dipole model is also used to calculate impedance of the slot antenna. Input impedance of the dipole antenna is changing by its length. Thus, impedance of the slot aperture will vary with respect to the slot length.. It is shown in [14] that if the length of the dipole is set almost one wavelength ($\sim 0.925\lambda$), input impedance of the dipole would be nearly 710 Ω. After this calculation, slot antenna input impedance can be computed by using the Babinet's principle as follows

$$Z_s = \frac{{Z_0}^2}{4Z_d} = \frac{35476}{Z_d} = 50\ \Omega \qquad (1)$$

where Z_0 is the intrinsic impedance of the free space, Z_s is the input impedance of the slot antenna and Z_d is the input impedance of the complementary dipole antenna.

However, it should be noticed that this equation is valid for slots which are etched from a metallic ground plane in air and fed with a delta gap source at the middle. Thus, equation (2) is not valid for the stripline fed slot antenna. However, basic designs are performed by considering this equation since it gives an idea related to length of the slot and width of the stripline.

If the slot length is chosen half a wavelength instead one wavelength, input impedance at the slot center would be different than 50Ω. If the slot length is chosen different than one wavelength, then an offset distance should be given to the feed line with respect to center of the slot in order to match the antenna input impedance to the 50Ω feed line impedance. Schematic views of the feeding points are given in Figure 3.

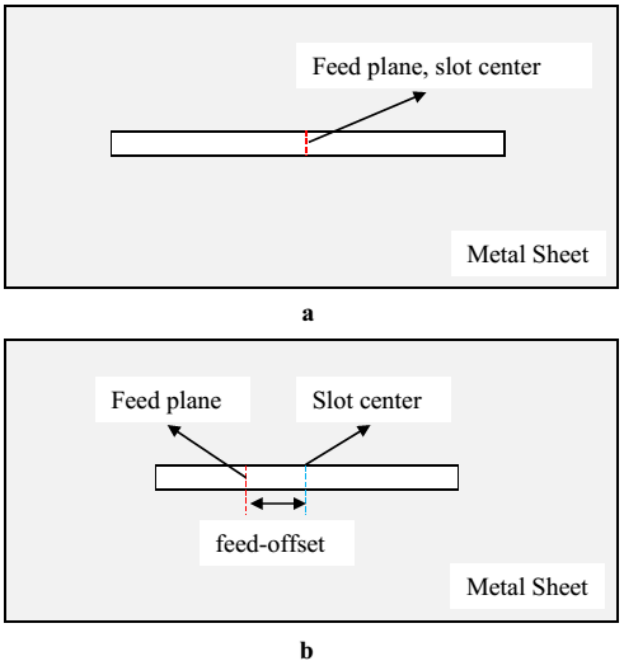

Figure 3 Schematic view of different slot length: a) one guided wavelength b) different from one guided wavelength

In order to feed the antenna at slot center, one wavelength is chosen as slot length, and it is calculated by means of equation given by [15]:

$$\lambda_g = \frac{c}{f\sqrt{\mu_r \varepsilon_r}} \cong 77\ mm \qquad (2)$$

where c is speed of the light in free space, f is desired resonant frequency, ε_r is the relative permittivity of the dielectric substrate and μ_r is the relative magnetic permeability of the dielectric substrate.

It should be noticed that this equation is valid for stripline structures where inner feed line is embedded in a dielectric material. However, Equation (2) is written for a slot which is not embedded in a dielectric material. One side of this slot is in the air. Thus, this equation is not valid for the stripline fed slot antenna. However, the value found from (2) is used as an initial value for simulations during design.

Stripline feed stuructre consists of 3 conductor layers, one of them is inner conductor and others are ground conductors that are connected to outer casing of the feeding connector. Internal conductor is embedded in a homogeneous and isotropic dielectric whose relative dielectric constant is ε_r [16]. Schematic view of the stripline feed structure is shown in Figure 4 a.

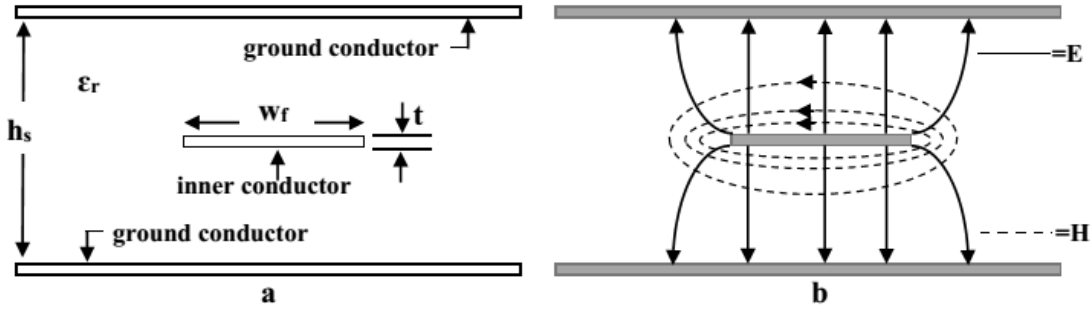

Figure 4 Schematic view of, a) strip line feed, b) field distribution

Electric field (**E**) and magnetic field (**H**) lines in the stripline feed structure are shown in Figure 4-b in a certain cross-section and at a certain time. Characteristic impedance of the stripline, Z_c, can be computed by the equation (3) which is given in [15]:

$$Z_c = \frac{Z_0}{2\pi\sqrt{\varepsilon_r}} \ln\left\{1 + 0.5\frac{8h_s}{\pi w_f'}\left[\frac{8h_s}{\pi w_f'} + \sqrt{\left(\frac{8h_s}{\pi w_f'}\right)^2 + 6.27}\right]\right\} \qquad (3)$$

where,

$$w_f' = w_f + \frac{\Delta w_f}{t} t \tag{4}$$

$$\frac{\Delta w_f}{t} = \frac{1}{\pi}\left\{1 - 0.5 \ln\left[\left(\frac{1}{2h_s/t + 1}\right)^2 + \left(\frac{1/4\pi}{w_f/t + 1.1}\right)^m\right]\right\} \tag{5}$$

and

$$m = \frac{6}{3 + \frac{2t}{h_s}} \tag{6}$$

w_f is the width of the stripline, h_s is the height of the substrate, Z_0 is the intrinsic impedance of the free space, t is the thickness of the conductor and ε_r is the relative permittivity of the dielectric substrate

Detailed information of the characteristic impedance derivations can be found in [15]. In this study, characteristic impedance of the stripline is estimated by using the tools of CST Microwave Studio®. An electromagnetic simulation is carried out in order to find the width of the stripline which corresponds to the characteristic impedance of 50 ohm. In this simulation, excitation ports are defined at the beginning and end of the stripline. Furthermore insertion loss and field distributions around the inner conductor are calculated. Simulation results show that characteristic impedance of the stripline is roughly found as 50 ohm when the width of the feed line is chosen as 1 mm. Electric and magnetic field distributions over the stripline feed are given in Figure 5 and Figure 6.

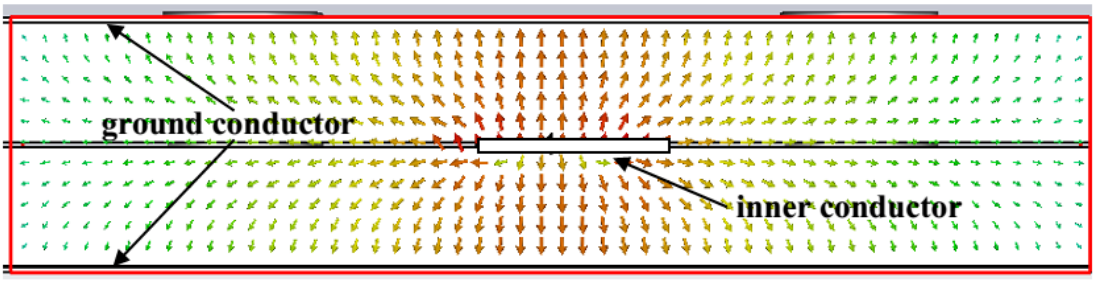

Figure 5 Electric field distribution surrounding of the stripline

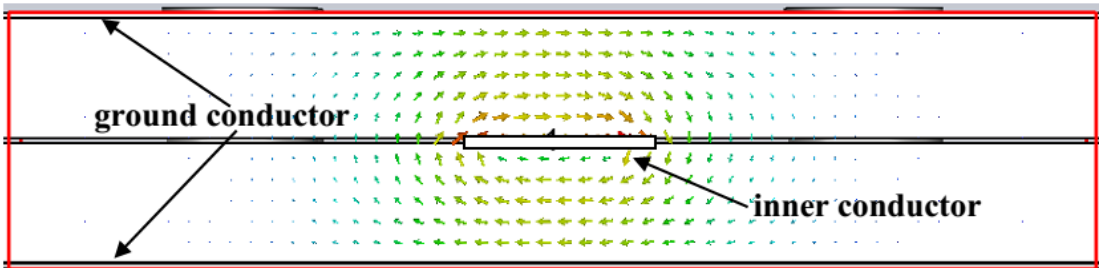

Figure 6 Magnetic field distribution surrounding of the stripline

It is observed from Figure 5 and Figure 6 that electric and magnetic field distributions over the port are found as expected. In order to obtain the loss over the stripline whose length is approximately $1.5\lambda_g$, S_{21} of the feed structure is calculated. Result of the simulation is given in Figure 7.

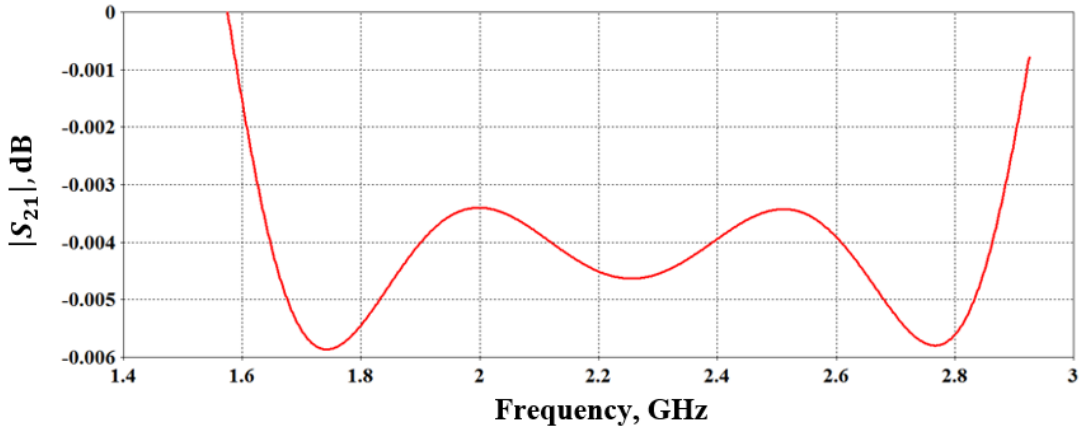

Figure 7 $|S_{21}|$ of the stripline feed

It is easily seen from Figure 7 that loss of stripline is very low. However, it should be noticed that parallel plate modes can be excited between the top and bottom ground conductors. In order to prevent these unwanted modes, small conductor bars (vias)

which provide electrical contact between the top and bottom conductors can be placed in the design, [16].

At the initial design phase of the stripline fed rectangular shaped slot antenna, which is called SFSA, length of the slot aperture (L_s) and width of the stripline (W_f) are determined as 77 mm and 1 mm, respectively. Also, vias are placed between the top and bottom ground conductors in order to prevent parallel plate mode excitations. Views of the SFSA obtained from the CST Microwave Studio® are given in Figure 8 and Figure 9.

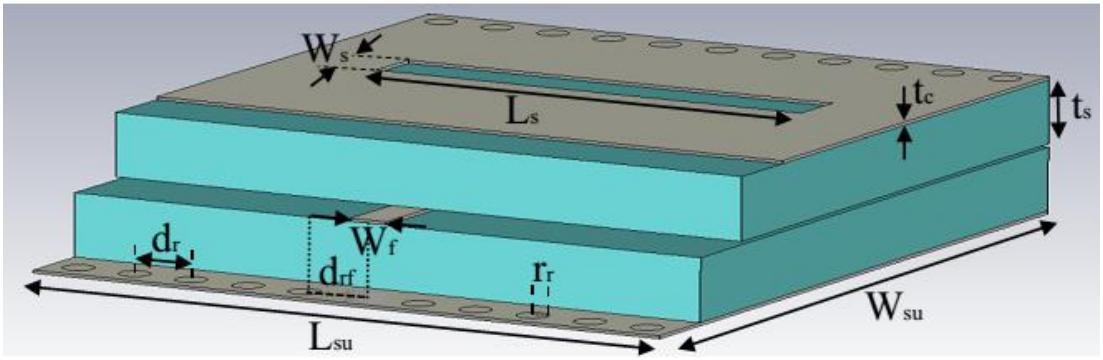

Figure 8 Sectional view of the designed SFSA

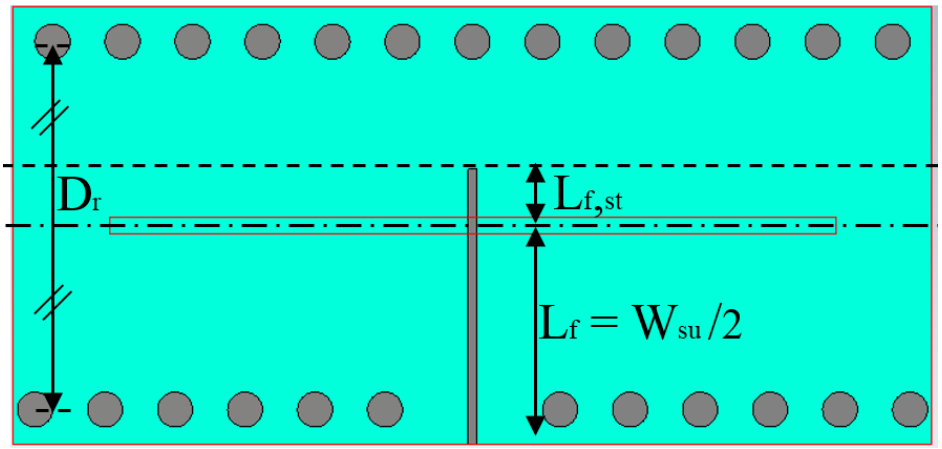

Figure 9 Top view of the designed SFSA (without top ground plane)

Based on the experience obtained by parametric study, antenna is designed and final values of parameters of antenna are given in Table 2. S_{11} result of the designed antenna is plotted as a function of frequency in Figure 10.

Table 2 Parameters of the SFSA

Parameters	**Description**	**Values (mm)**
W_{su}	Width of each substrate	50
L_{su}	Length of each substrate	105
W_f	Width of feed	1
L_f	Length of feed	25
$L_{f,st}$	Length of feed stub	6.5
W_s	Width of slot	2
L_s	Length of slot	74
r_r	Radius of vias	0.5
d_r	Distance between centers of vias	4
d_{rf}	Distance between center of nearest via and center of the feed line	2
D_r	Distance between centers of upper and lower vias	42

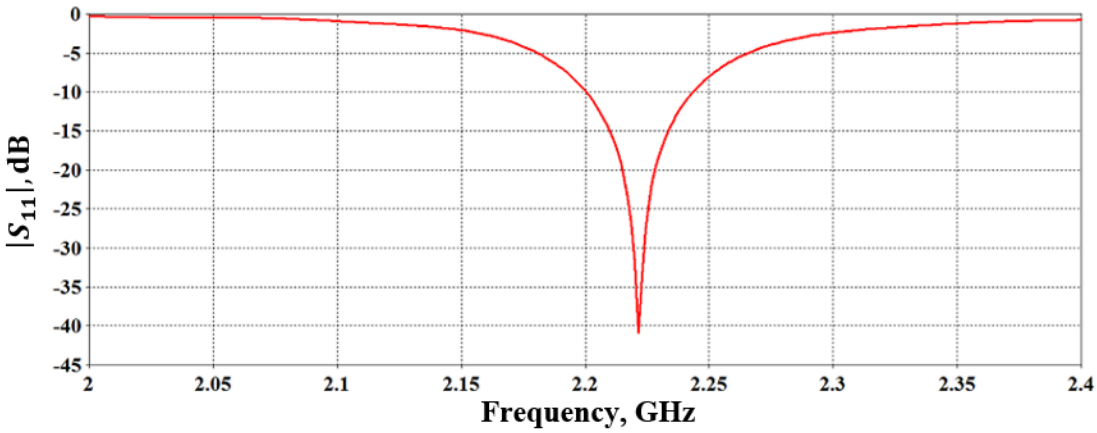

Figure 10 S_{11} of the SFSA

It is seen from Figure 10 that resonance frequency of the SFSA is 2.22 GHz, $|S_{11}|$ value at the center frequency is -41 dB and 10dB bandwidth is 43 MHz.

Polar plot and 3-D radiation pattern obtained by simulation are given in Figure 11 and Figure 12.

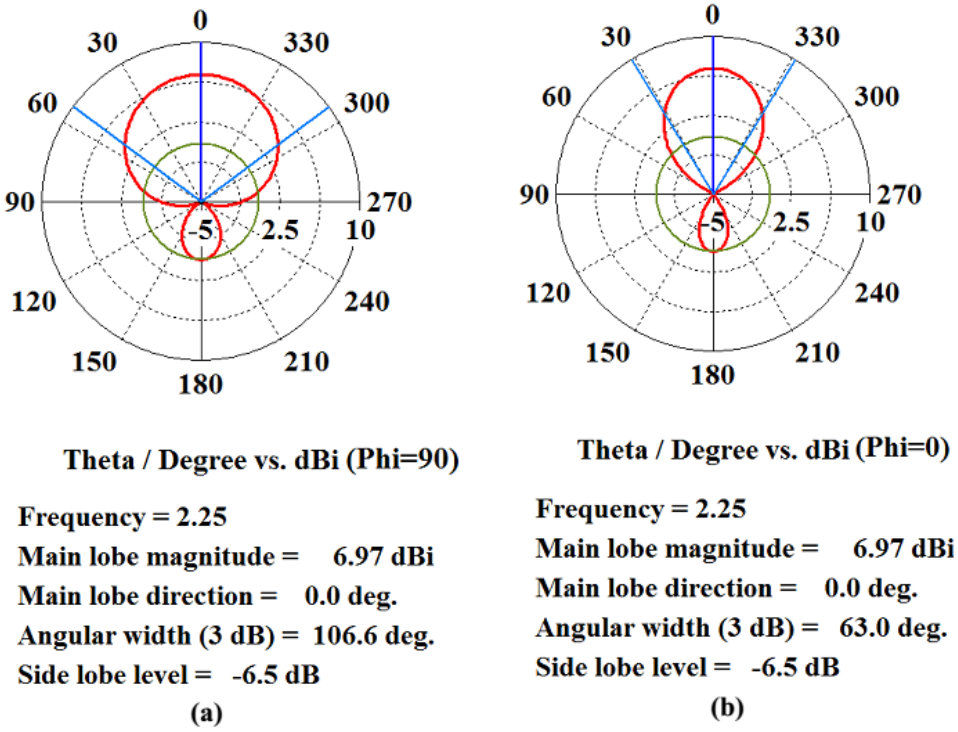

Figure 11 Far field of SFSA, a) E-plane, b) H-plane

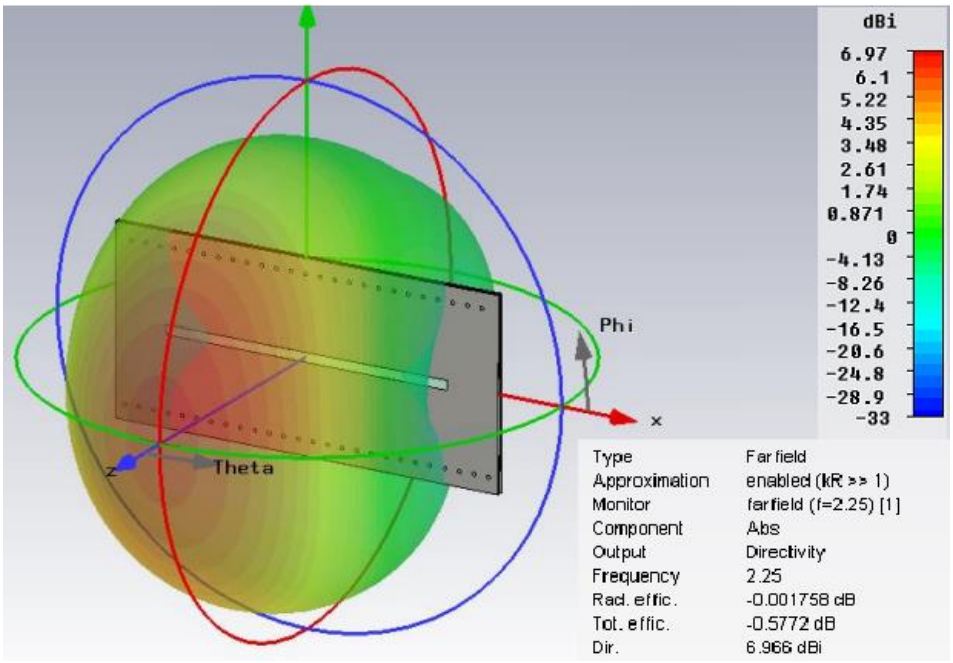

Figure 12 3-D view of the far-field pattern

2.3 Parametric Study of SFSA

To understand the effect of each parameter on the antenna performance, parametric study is performed. To examine the effect each parameter, the other parameters of the antenna are kept as in Table 2 whole changing the value of examined parameter in a certain range. Effects on the antenna input return loss characteristics are observed.

1. Effect of length of the slot, L_s

Length of the slot is one of the most critical parameter that controls the resonance frequency. L_s is changed from 71 mm to 83 mm by 3 mm steps. Magnitude of S_{11} versus frequency curves are plotted on Figure 13.

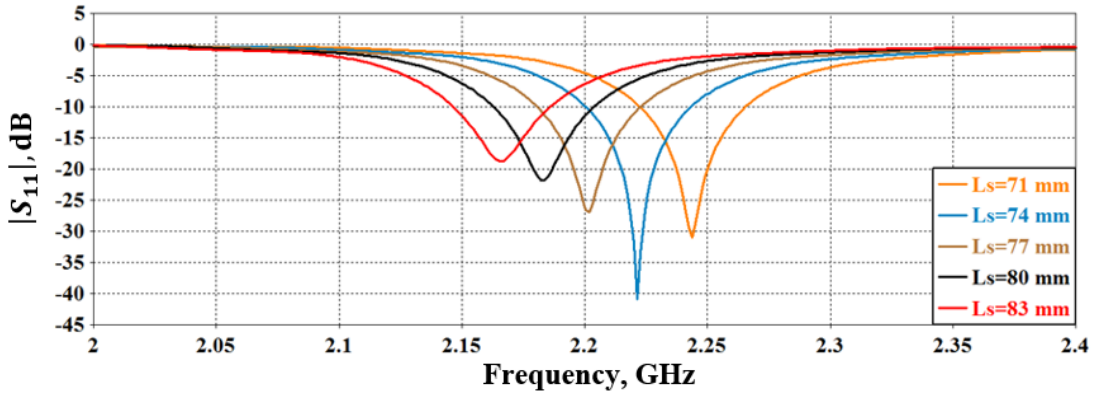

Figure 13 $|S_{11}|$ versus frequency plots for different L_s values

It is seen from Figure 13 that operating frequency of the antenna is directly controlled by the slot length.

2. Effect of width of the slot, W_s

Another parametric study is achieved for the width of the slot. Slot width, W_s, is changed from 1 mm to 3 mm by 0.5 mm steps. Magnitude of S_{11} is plotted for each W_s on Figure 14.

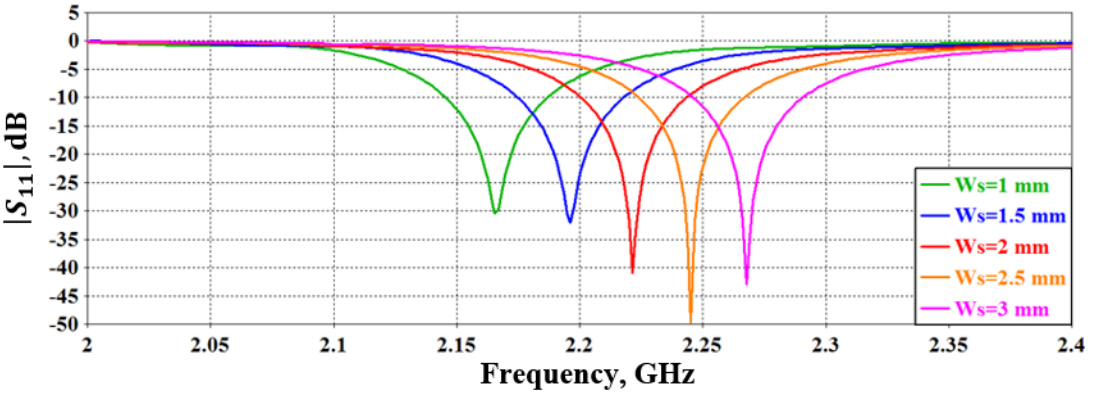

Figure 14 $|S_{11}|$ versus frequency plots for different W_s values

It is observed from figure that operating frequency shifts up when value of W_s is increased. Antenna tends to have wider bandwidths for wide slot widths, however working frequency is shifting to upper frequency and amplitude of S_{11} is decreasing.

3. Effect of feed stub length, $L_{f,st}$

Feed stub length (*see Figure 9*) plays an important role in the matching of the slot input impedance and stripline impedance. Length of the feed is adjusted as half of the substrate width. However, it is needed to add a stub line to the feed in order to match slot input impedance and stripline impedance. The length of the stub is changed between 5.5 mm to 7.5 mm by 0.5 mm steps. Obtained S_{11} values are plotted in Figure 15. It is observed that magnitude of S_{11} reaches the smallest value when $L_{f,st}$ is around 6.5 mm.

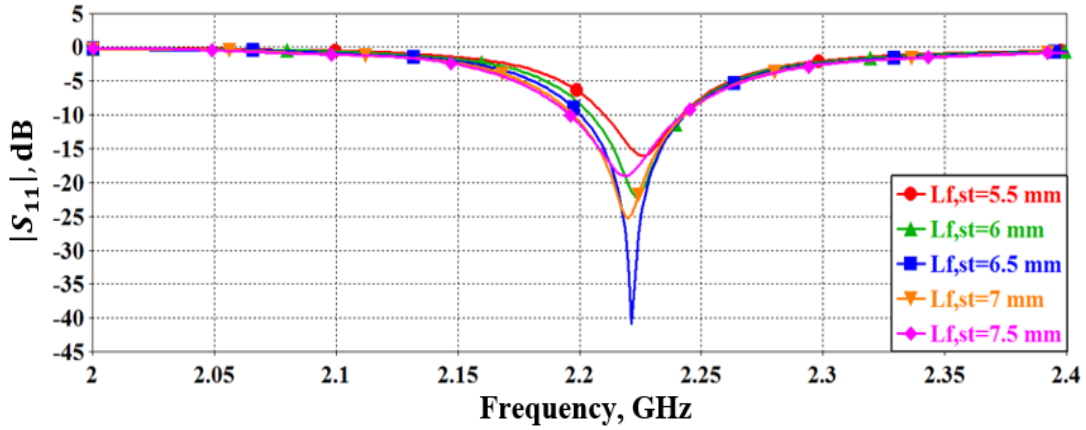

Figure 15 $|S_{11}|$ versus frequency plots for different $L_{f,st}$ values

It is observed that $L_{f,st}$ can be used to match the antenna 50 Ω.

4. Effect of d_r

Another parametric study is carried out for the distance between the centers of vias (d_r) while other parameters given in Table 2 are left same. $|S_{11}|$ values obtained from the simulation are shown on Figure 16.

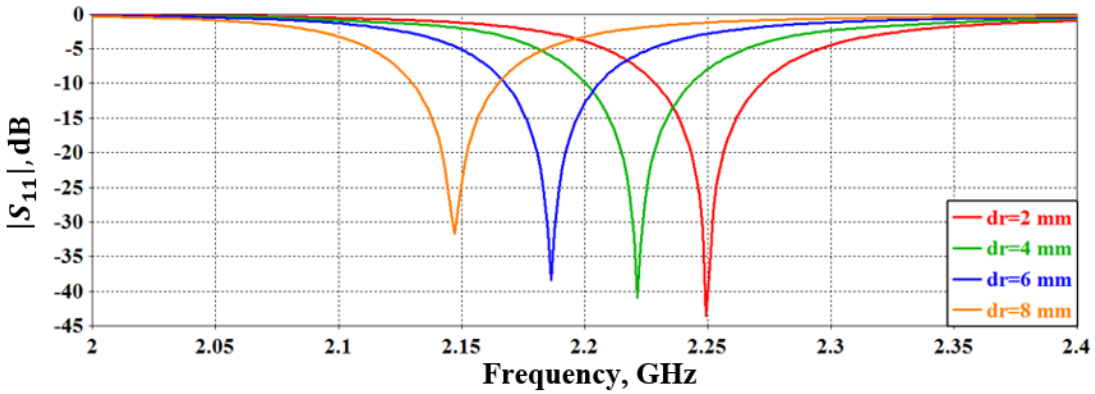

Figure 16 $|S_{11}|$ versus frequency plots for different d_r values

It is observed from Figure 16 that d_r affects the resonance frequency. When d_r decreases, resonance frequency increases. Bandwidth of the antenna for each d_r is tabulated in Table 3. Table shows that bandwidth of the antenna gets smaller when the distance between the centers of vias (d_r) is raised.

Table 3 10 dB bandwidth values for different d_r

d_r (mm)	Bandwidth (MHz)
2	45
4	43
6	38
8	35

5. Effect of D_r

This parametric study is performed to observe the effects of the change in the distance between the centers of upper and lower rows of vias (*see Figure 9*). It should be noticed that rows of vias are placed at the upper and lower sides of the antenna so that distance between the centers of upper / lower vias and center of the slot are equal to each other (*see Figure 9)*. Magnitudes of S_{11} for D_r values are plotted in Figure 17.

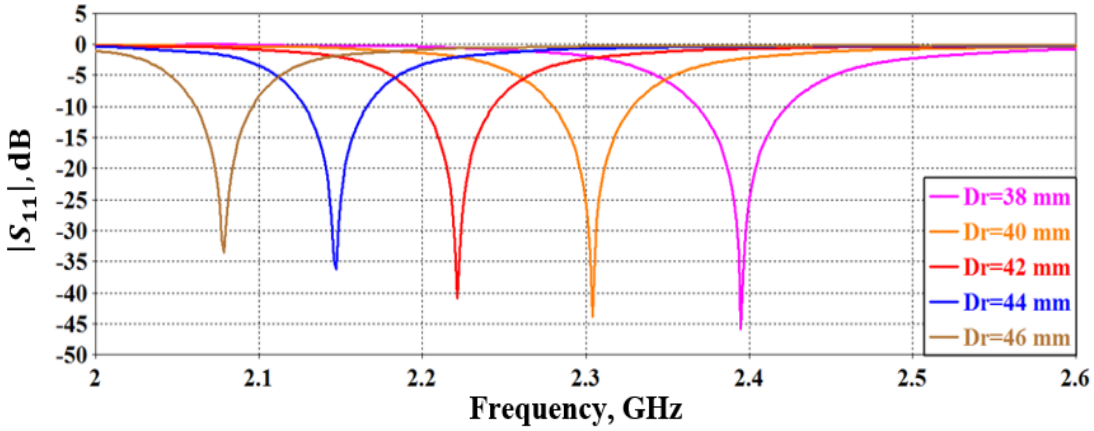

Figure 17 $|S_{11}|$ versus frequency plots for different D_r values

It is observed from Figure 17 that resonance frequency of the antenna increases as D_r. Besides, Table 4 shows that bandwidth of the antenna gets wider as D_r is decreased.

Table 4 10 dB bandwidth values for different D_r

D_r (mm)	Bandwidth (MHz)
38	55
40	49
42	43
44	39
46	35

2.4 Fabrication and Measurement

Designed antenna is fabricated using PCB prototyping machine. Fabrication process is started by producing two layers of the antenna and it is continued by integrating these separate layers. Top layer has a slot on one side, whereas feed line on the other side. Bottom layer is just a grounded dielectric layer. In both layers vias are drilled and electroplated. Some modifications are done on the designed antenna to integrate two separate dielectric layers. In order to assemble these layers, they are soldered to each other. Rectangular shaped gaps shown in Figure 18 are located at the suitable

place over the dielectric layer for soldering operation. Substrate width is increased since there is no sufficient space over the substrate layer. In addition, lower side of the top dielectric and upper side of the bottom dielectric are covered with the frame shaped conducted plate for providing the electrical continuity between the top and bottom ground layers. It should be indicated that this electrical conductivity is provided by using vias in the simulation. These modifications can be easily seen from Figure 18, Figure 19 and Figure 20.

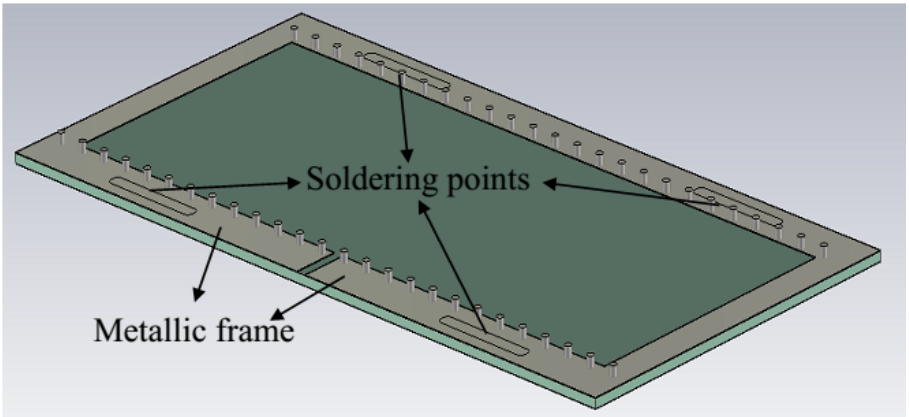

Figure 18 View of the bottom substrate in simulation

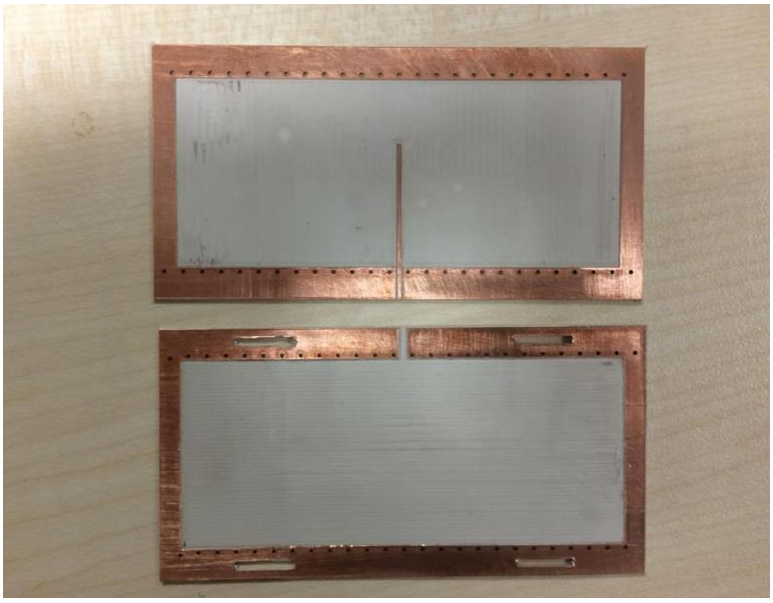

Figure 19 Metallic frames of the fabricated antenna

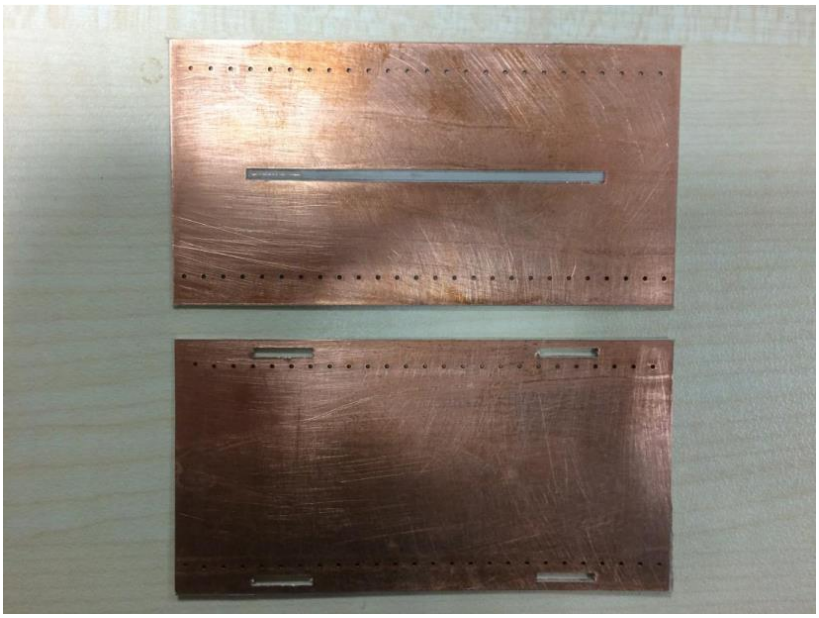

Figure 20 Top and bottom ground plates of the fabricated antenna

Furthermore, view of the fabricated antenna which is formed by integrating top and bottom layers is given in Figure 21.

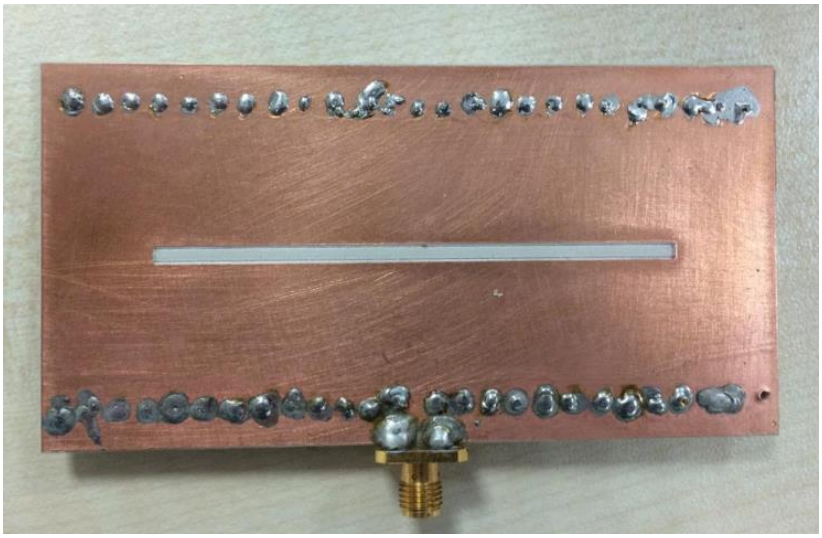

Figure 21 View of the fabricated antenna

In order to compare the designed and fabricated antenna results, bandwidth and S_{11} of the antenna are measured. Measurement results are given together with simulation

results in Figure 22. It is observed that resonance frequency obtained by simulations and measurements are same. However, loss in the frequency band 2-2.4 GHz is more than expected. It is needed to design a mold to tightly integrate two layers to each other. If the layers are not tightly combined, air gaps are taken place between the top and bottom layers. These air gaps disturb the antenna $S_{11}$when someone is getting close to antenna or touches it. Thus, layers are hardly fastened, and soldered to each other. Vias are second issue since they are not covered by copper during the plating through-hole process. Therefore, each via hole is soldered after the layers are integrated. This soldering process takes much more time and it also causes disturbance in S_{11} and bandwidth depending on the human ability. It is needed to improve a method instead of the one by one soldering each hole. Due to these problems, S_{11} characteristic of the fabricated antenna is found as worse than the one for designed antenna.

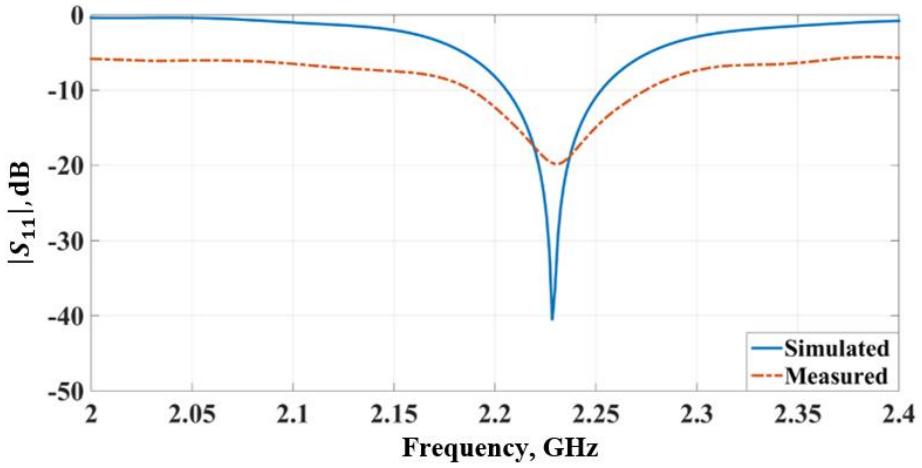

Figure 22 Return loss of the fabricated and simulated antenna

Bandwidth and S_{11} measurement results of the simulated and fabricated antennas are listed in Table 5.

Table 5 S_{11} and bandwidth measurement results

	S_{11} (dB)	**Bandwidth (MHz)**
Simulated Antenna	-42	43
Fabricated Antenna	-17	45

Table shows that bandwidth values of the fabricated and simulated antenna are so close to each other.

Furthermore, fabricated antenna radiation patterns are also measured in the principle planes. These measurements are performed in the anechoic chamber located at METU EEE Department. Measured radiation patterns are plotted in E & H planes in Figure 23.

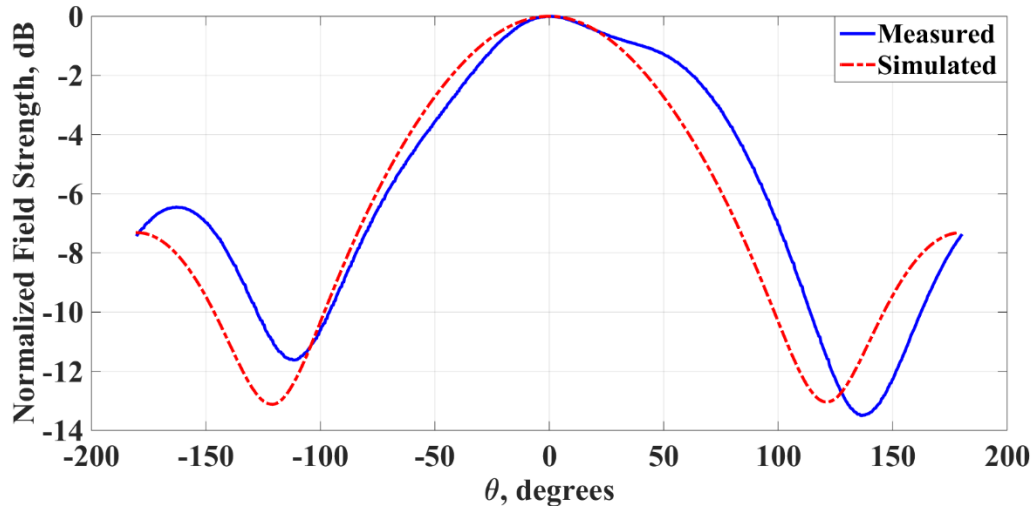

(a)

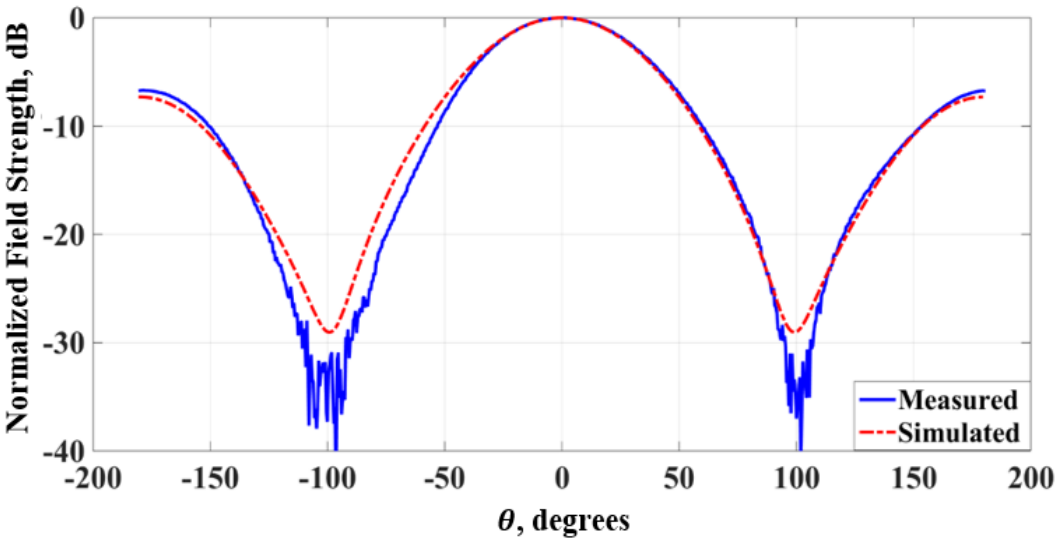

(b)

Figure 23 Normalized radiation patterns of the simulated and fabricated SFSA: (a) E-plane, (b) H-plane

It can be easily seen from Figure 23 that far-field patterns obtained by measurement and simulations agree well with each other.

Measurement result shows that bandwidth of the fabricated antenna does not meet the defined requirement. Wider bandwidth can be obtained by modifying the slot shape in Chapter 3. Design fabrication and measurement procedures of SFSA with rounded bow-tie slot are presented.

CHAPTER 3

DESIGN, FABRICATION AND MEASUREMENT OF A STRIPLINE FED ROUNDED BOW-TIE SHAPED SLOT ANTENNA

In the previous chapter, it is clearly seen that SFSA does not satisfy the bandwidth requirement given in section 2.2. Thus, it is decided to design a new antenna which has a wider bandwidth. Design, fabrication and measurement studies of this new antenna are explained in this chapter. Slot shape and feed structure of the antenna is modified to obtain wider bandwidth. These modifications are performed by considering the parametric studies. Design procedure and parametric calculations related to modified slot shape and feed structure are mentioned in section 3.1 and 3.3, respectively. Although there are some small differences in the fabrication process, designed antenna is produced in a similar manner as in Chapter 2. Comparisons between the simulation results and measurements are given in section 3.4.

3.1. Design of Stripline Fed Rounded Bow-Tie Shaped Slot Antenna

It is obvious that bandwidth of the SFSA should be increased to meet the desired design requirements. In order to achieve this purpose, similar studies in the literature are investigated. It is shown in [6] that the size of the slot section should be increased to obtain a wider bandwidth. Therefore, it is intended to change geometry of the rectangular shaped slot. In order to make a decision related to shape of the aperture, surface current distribution around the slot section can be considered. View of the surface current distribution is given in Figure 24.

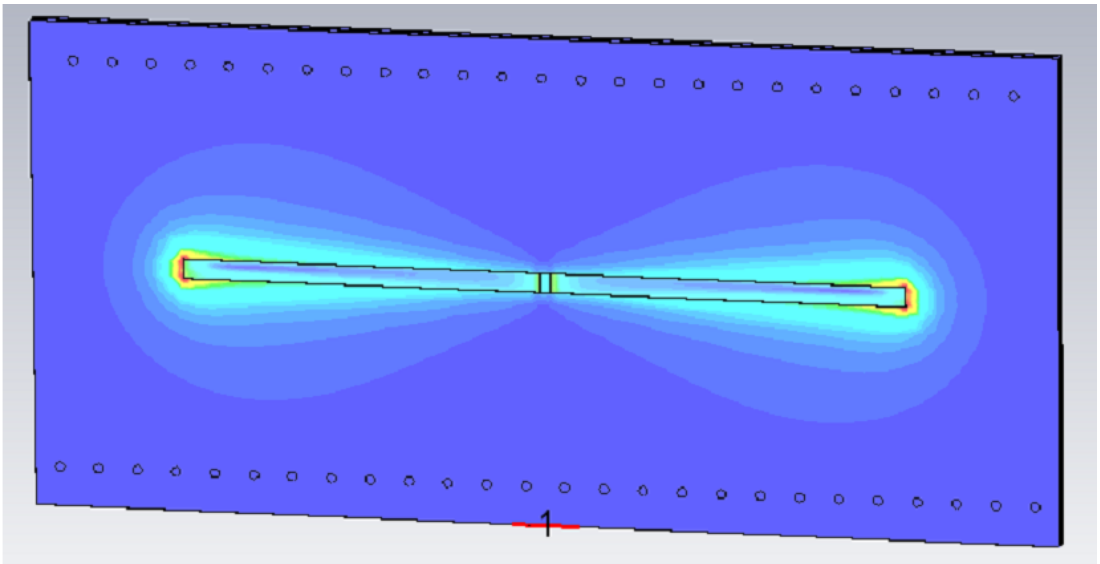

Figure 24 Surface current distribution around the slot section

Figure 24 clearly shows that shape of new slot can be chosen as rounded bow-tie. This antenna is named as Stripline Fed Rounded Bow-Tie Shaped Slot Antenna (SFRSA). Shape of the slot of the antenna is given in Figure 25.

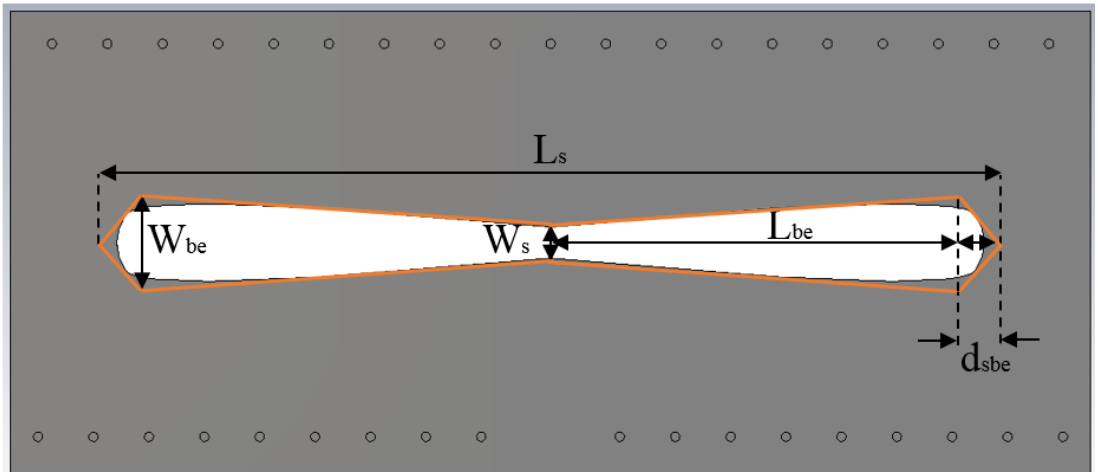

Figure 25 Front view of the designed SFRSA

SFRSA can be designed by using the information obtained from section 2.2. It is a fact that some design parameters used in the previous chapter are left same, since only the shape of the slot is modified. In addition to parameters of the SFSA, some new parameters given in Table 6 are placed to design. Furthermore, it is noticed that

rounded slot structure is drawn by means of the orange lines in the simulation tool (*see Figure 25*), so new parameters should be defined as considering these guidelines. Due to this reason, L_s (length of the slot) is not equal to the real slot length. However, this situation is just valid for the length of the slot (L_s), width of the rounded section (W_{be}) and length of the rounded section (L_{be}). Difference between the real and drawn dimensions is smaller than one millimeter.

It is also needed to perform parametric studies for some parameters in order to show relation between the physical dimensions and their effects on the radiation characteristics of the antenna such as S_{11} and bandwidth. Designed antenna parameters are given in Table 6.

Table 6 Parameters of the SFRSA

Parameters	**Description**	**Values (mm)**
W_{su}	Width of each substrate	50
L_{su}	Length of each substrate	117
W_f	Width of feed	1
L_f	Length of feed	25
$L_{f,st}$	Length of feed stub	7
W_s	Width of slot	3.4
L_s	Length of slot	96
L_{be}	Length of the rounded section	44
W_{be}	Width of the rounded section	6
r_r	Radius of conducted rods	0.5
d_r	Distance between centers of the vias	6
d_{rf}	Distance between the centers of nearest via and the feed line	7.5
$D_{r,u}$	Distance between the centers of the slot and upper vias	21.5

$D_{r,l}$	Distance between the centers of the slot and lower vias	21

Magnitude of S_{11} versus frequency plot of SFRSA designed by considering these parameters is given in Figure 26.

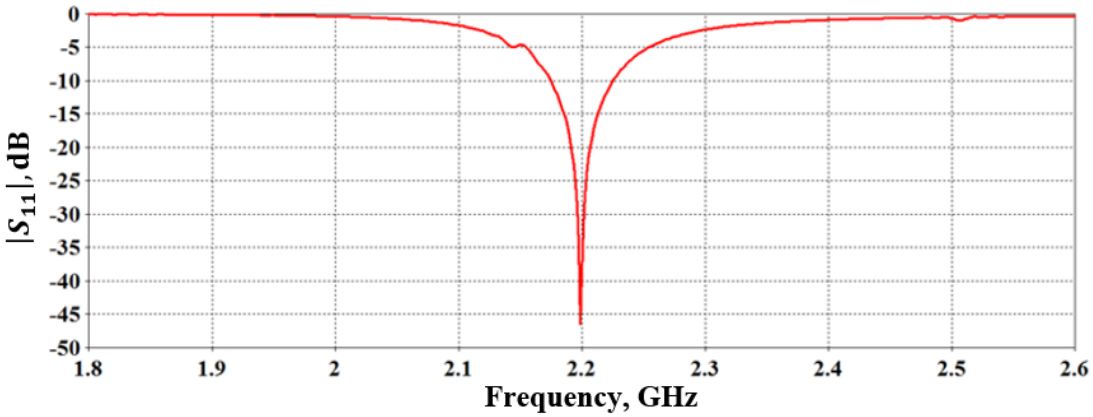

Figure 26 S_{11} of the SFRSA

It is easily seen from Figure 26 that return loss and bandwidth of the SFRSA are approximately 46 dB and 51 MHz, respectively.

Far-field patterns of the antenna in polar form are given in Figure 27. Three dimensional view of the far field pattern is also shown in Figure 28.

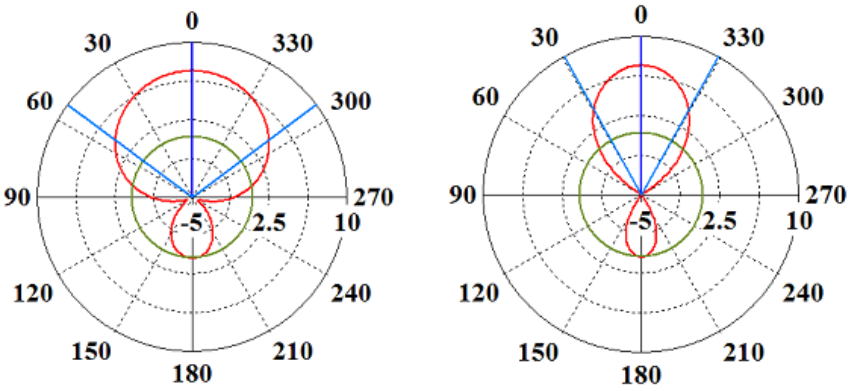

Theta / Degree vs. dBi

Frequency = 2.25
Main lobe magnitude = 7.24 dBi
Main lobe direction = 0.0 deg.
Angular width (3 dB) = 106.7 deg.
Side lobe level = -6.3 dB

(a)

Theta / Degree vs. dBi

Frequency = 2.25
Main lobe magnitude = 7.24 dBi
Main lobe direction = 0.0 deg.
Angular width (3 dB) = 58.1 deg.
Side lobe level = -6.3 dB

(b)

Figure 27 SFRSA far field (a) E-plane (b) H-plane

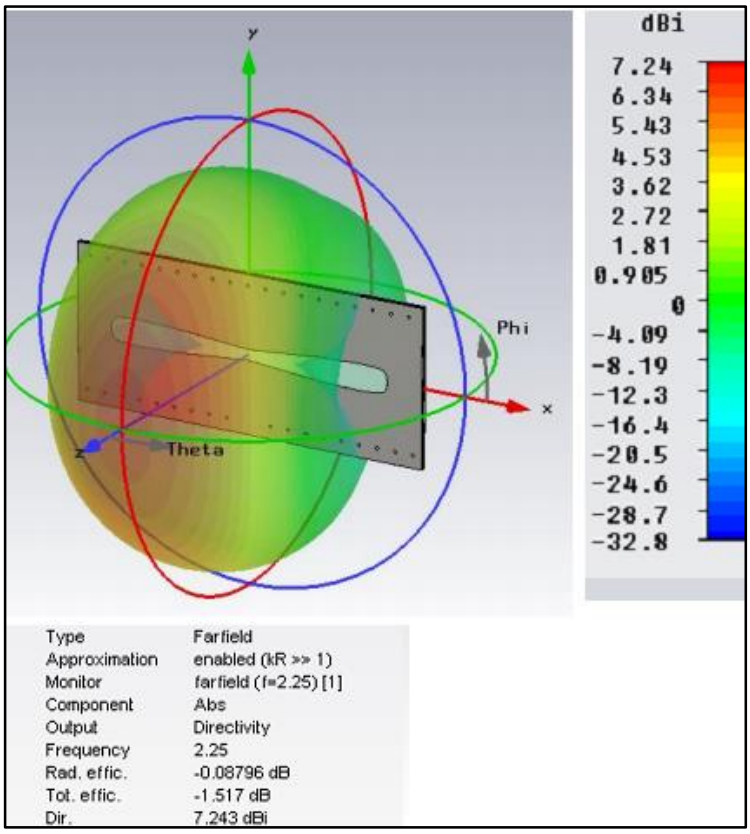

Figure 28 3-D view of the far-field

Results of these simulations show that SFRSA satisfies the bandwidth requirement, but it is too close to limit value of given requirement. To improve the bandwidth, propose antenna structure is modified as explained in section 3.2.

3.2. Parametric Study of SFRSA

Parametric calculations are performed for this antenna from similar reasons in section 2.3.

1. Effect of slot length, L_s

First parametric study is performed for the length of the slot. However, length of the slot is both depending on L_{be} and d_{sbe}, in this design. Thus, d_{sbe} can be chosen as a constant parameter for each simulation and $L_s/2$ can be changed with certain steps. For instance, if this constant distance (d_{sbe}) is adjusted as 4 mm, it means that L_{be} and $L_s/2$ is equal to 36 mm and 40 mm, respectively. It is decided to make parametric calculations for L_s and L_{be} where d_{sbe} is equal to 2, 4 and 6 mm, respectively. Simulation results of this study are given in Figure 29, Figure 30 and Figure 31 in terms of S_{11}.

first run for d_{sbe}=2 mm;

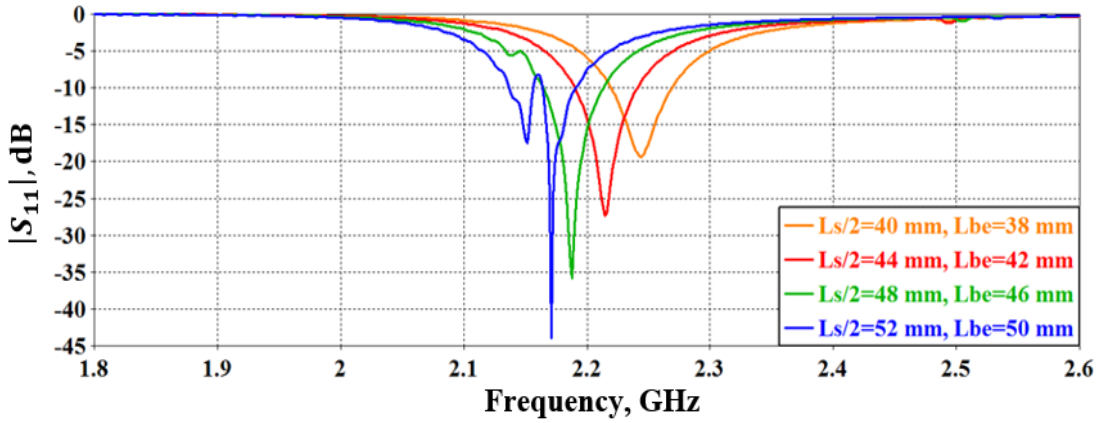

Figure 29 S_{11} of the SFRSA with respect to L_s and L_{be}

second run for d_{sbe}=4 mm;

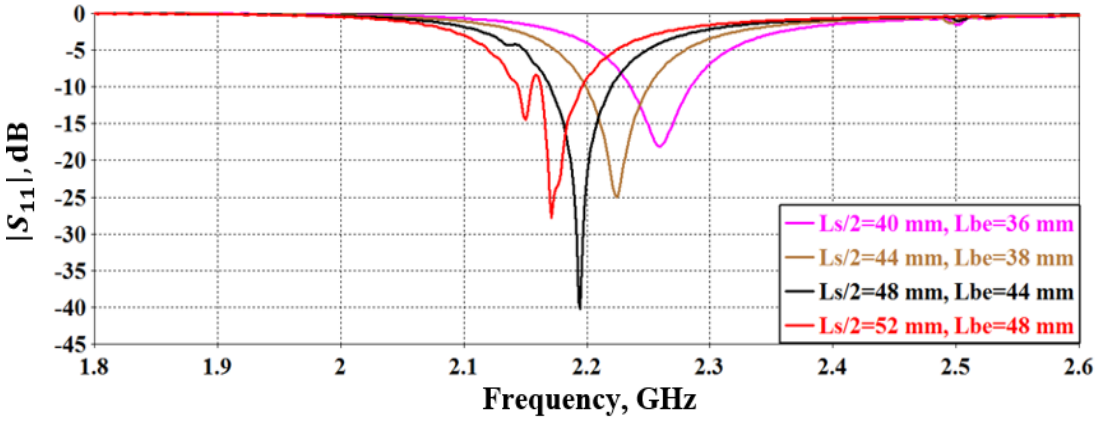

Figure 30 S_{11} of the SFRSA with respect to L_s and L_{be}

third run for d_{sbe}=6 mm;

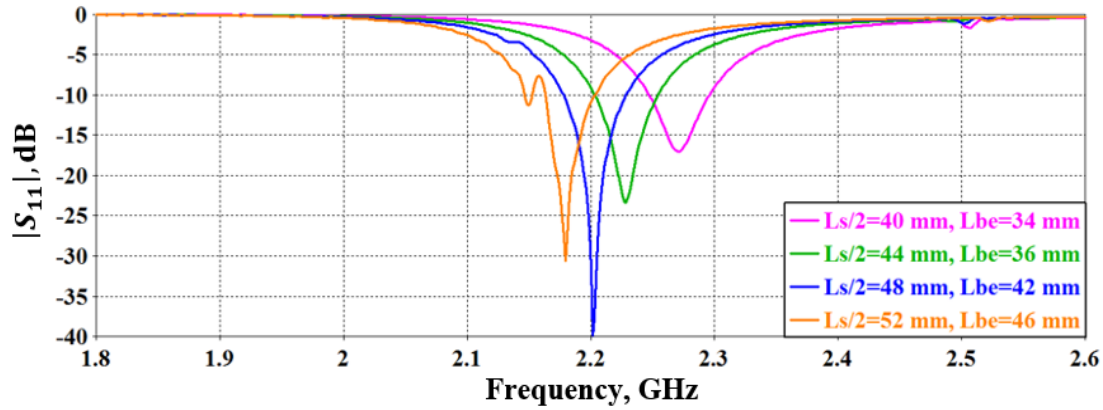

Figure 31 S_{11} of the SFRSA with respect to L_s and L_{be}

It is observed from Figure 29, Figure 30 and Figure 31 that operating frequency of the antenna is around 2.2 GHz when $L_s/2$ is equal to 48 mm independent of d_{sbe}. Besides, Figure 30 shows that antenna S_{11} reaches the maximum value when L_{be} is equal to 44 mm.

2. Effect of slot width, W_s

In order to observe effects of the slot width on the return loss, parametric calculations are performed for W_s. Return loss versus frequency curves for different W_s values are given in Figure 32.

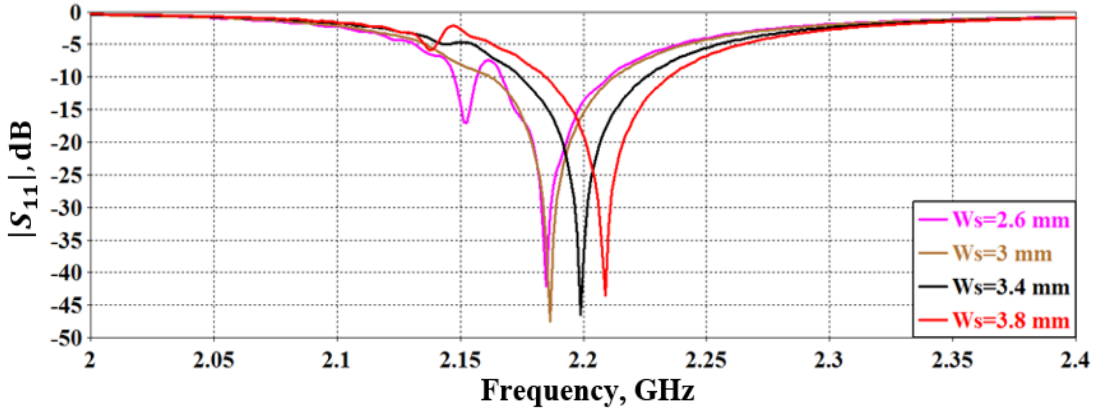

Figure 32 S_{11} of the SFRSA with respect to W_s

Figure 32 shows that operating frequency of the antenna is shifting towards the upper frequency band when the slot width is increased. It is seen from the figure that antenna bandwidth gets wider when the slot width is increased.

3. Effect of width of the rounded section, W_{be}

Another important parameter for the SFRSA is width of the rounded section that is a new parameter. $|S_{11}|$ of the antenna obtained by changing W_{be} is given in Figure 33.

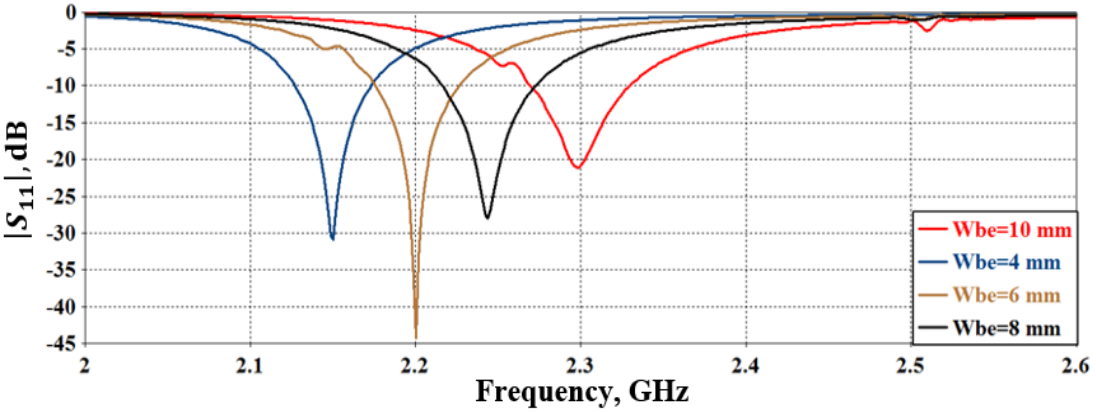

Figure 33 S_{11} of the SFRSA with respect to W_{be}

It is seen from Figure 33 that operating frequency of the antenna is shifting to upper frequency band when the width of the rounded section is increased. Shift in the frequency is occurred when W_{be} increases, i.e the upper and lower vias approach to the slot. It is believed that energy density around the slot is increasing when vias get closer the slot, and this causes an increment at the bandwidth. A wider bandwidth is obtained by increasing W_{be}, while operating frequency is shifting towards to upper band.

3.3. Design of the Broadband Stripline Fed Rounded Bow-Tie Shaped Slot

It is understood that SFRSA is barely met the bandwidth requirement. Thus, it needs some modifications over the SFRSA to obtain a wider bandwidth. These modifications and parametric calculations are presented in this section.

As mentioned at [17], a transverse stub can be added to feed structure to excite the antenna to introduce another resonance close to the operating frequency. This new antenna is called B-SFRSA (Broadband-SFRSA). Schematic view and new design parameters of the B-SFRSA, are given in Figure 34 and Table 7, respectively.

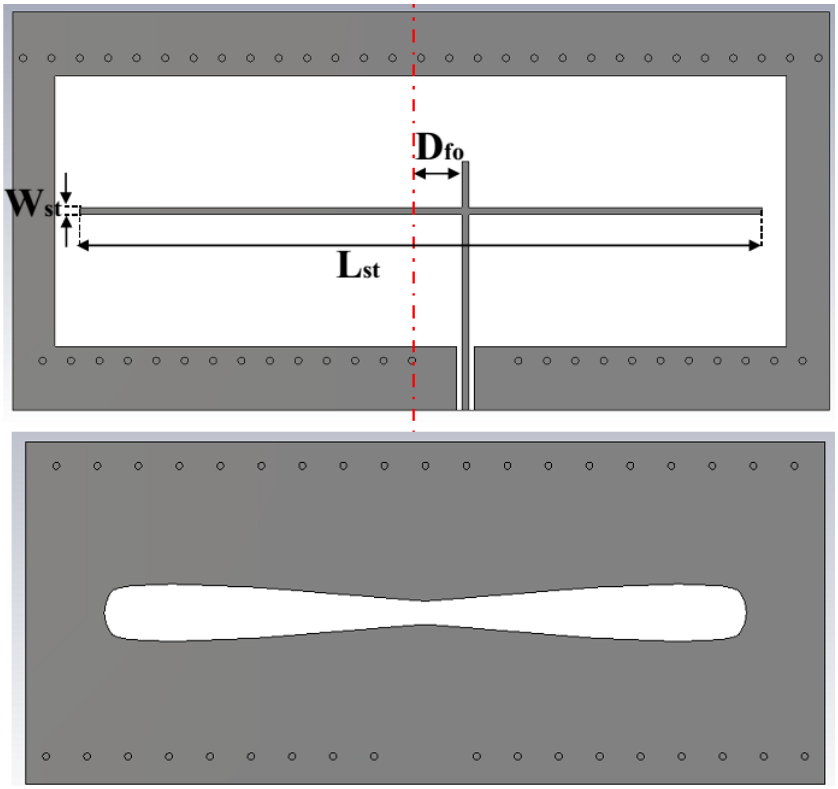

Figure 34 Geometry of slot layer and feed layer of the B-SFRSA

Table 7 Parameters of the B-SFRSA different than SFRSA

Parameters	**Description**	**Values (mm)**
L_s	Length of slot	100
L_{st}	Length of the stub	96
W_{st}	Width of the stub	1
d_r	Distance between centers of vias	4
D_{fo}	Distance of feed offset	4.5

In order to obtain a second resonance, B-SFRSA includes a long transverse stub structure added to stripline feed. This stub is placed at the middle of the slot section as being the same plane with the stripline feed. In this design, slot is not fed from the center to obtain good impedance matching between slot and feed line. To investigate

effects of stub, on radiation characteristics, parametric study is performed for the new parameters.

1. Effect of length of the stub, L_{st}

First parametric study is performed for length of the stub to show relation between second resonance and stub length. Magnitude of S_{11} versus frequency curves are plotted on Figure 35.

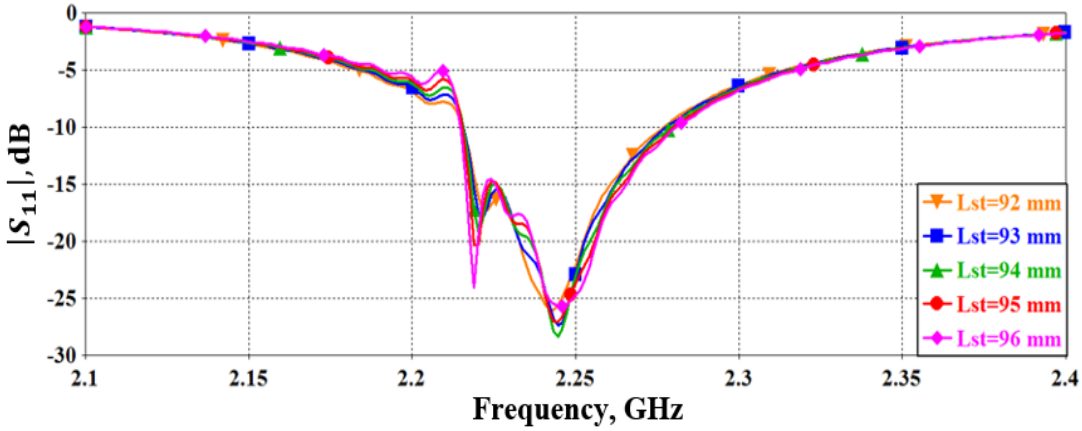

Figure 35 S_{11} of the B-SFRSA with respect to L_{st}

As seen from Figure 35, a second resonance occurs at frequency 2.22 GHz which is very close to the original one at 2.25 GHz by inclusion of the transverse stub.

It is seen from Figure 35 that all curves are almost have similar form but second resonance becomes more apparent when L_{st} increases.

2. Effect of distance of feed offset, D_{fo}

In the design of b-SFRSA, feed line is allowed to be moved from the center of the slot. Thus, the effects of the feed offset distance should be investigated. S_{11} values of the antenna for different offset values obtained from the parametric simulation are given in Figure 36.

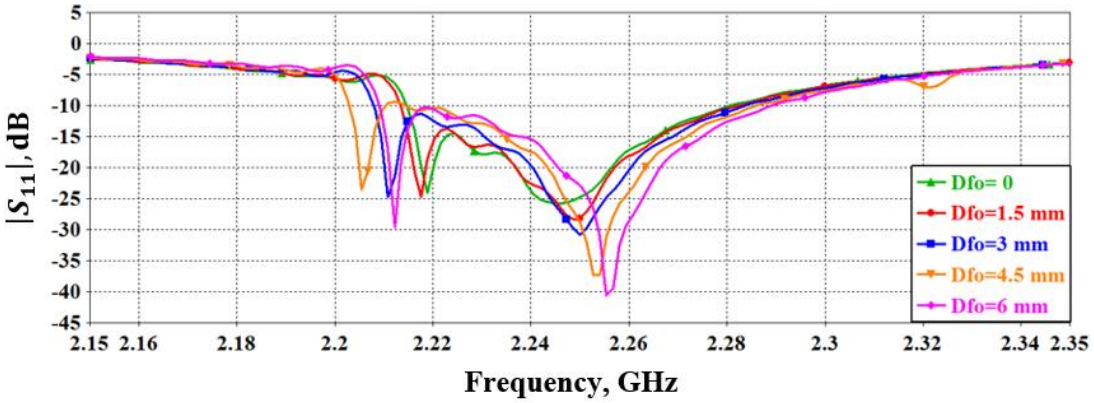

Figure 36 S_{11} of the B-SFRSA with respect to D_{fo}

It is observed from Figure 36 feed offset distance has an effect on bandwidth of the antenna. For the given simulation results, bandwidth is maximum when D_{fo} is equal to 4.5 mm. Adding a transverse stub to the feed structure affects the input impedance. To match the slot impedance to the feed line, feed line should be offset from the center.

3. Effect of width of the stub, W_{st}

Final parametric simulation is performed for the width of the stub to obtain its effects on the bandwidth. Results of the simulations in terms of S_{11} are given in Figure 37.

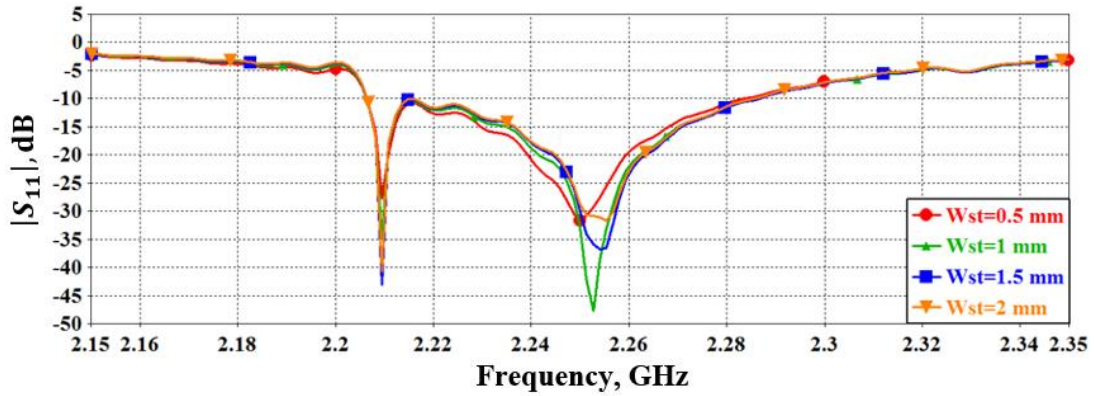

Figure 37 S_{11} of the B-SFRSA with respect to W_{st}

It is observed that, change of W_{st} does not significantly affect the radiation characteristics.

Based on the experience gained through parametric study B-SFRSA is designed. The dimensions are given in Table 7. Magnitude of S_{11} characteristics is plotted on Figure 38.

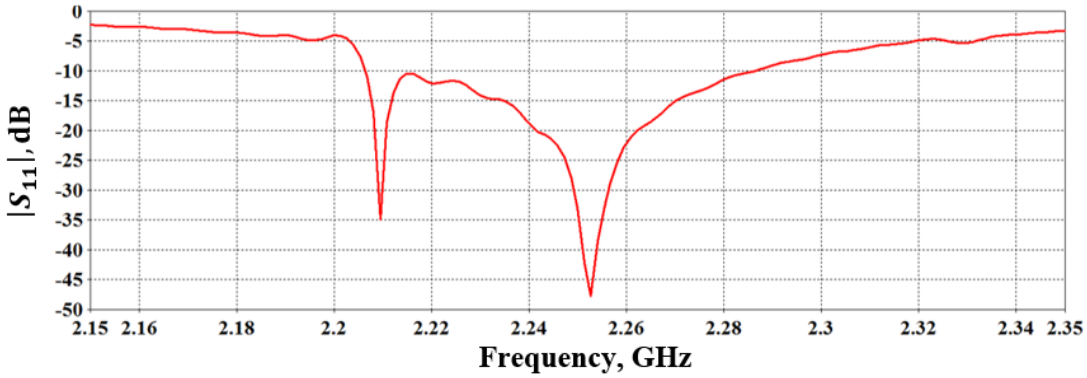

Figure 38 Bandwidth of the B-SFRSA

10 dB bandwidth of the B-SFRSA is nearly 80 MHz. Fabrication process of this antenna and comparisons between measured and simulated results are presented in section 3.4.

3.4. Fabrication and Measurement

Designed B-SFRSA is fabricated using simulation techniques explained in section 3.3. Additionally, press machine is used to combine two layers.

As explained in chapter 2, fabrication procedure consists of two main steps. First step is producing the printed circuit boards and the second step is integrating these separate boards to each other. In this antenna, press machine is used to assemble separate layers. A thin sheet of dielectric material is placed between the layers, and located in press machine. This machine applies both pressure and heat to the antenna for a few hours. As a result the separate layers are tightly integrated to each other since the dielectric material is fused them. Photographs of fabricated antenna are given in Figure 39, Figure 40 and Figure 41.

Figure 39 View of the fabricated layers inside

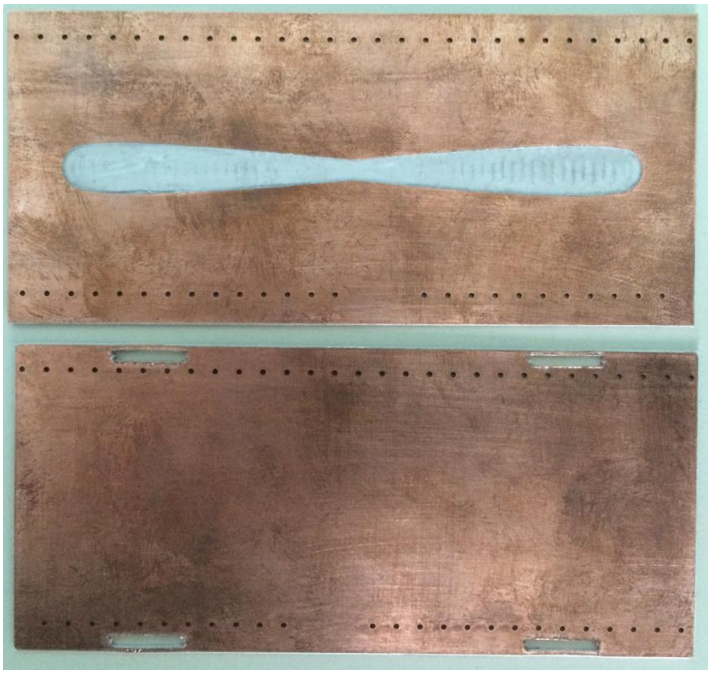

Figure 40 View of the fabricated layers outside

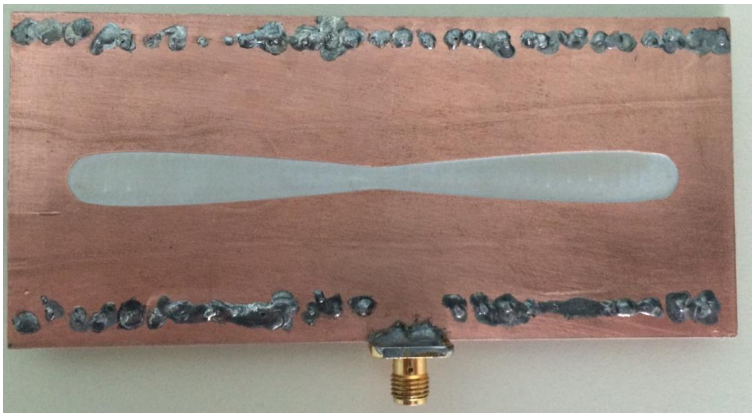

Figure 41 View of the fabricated antenna

Input return loss of the antenna is measured and compared with the simulation results in Figure 42. There is a shift of 60 MHz between the operating band of simulated and measured results.

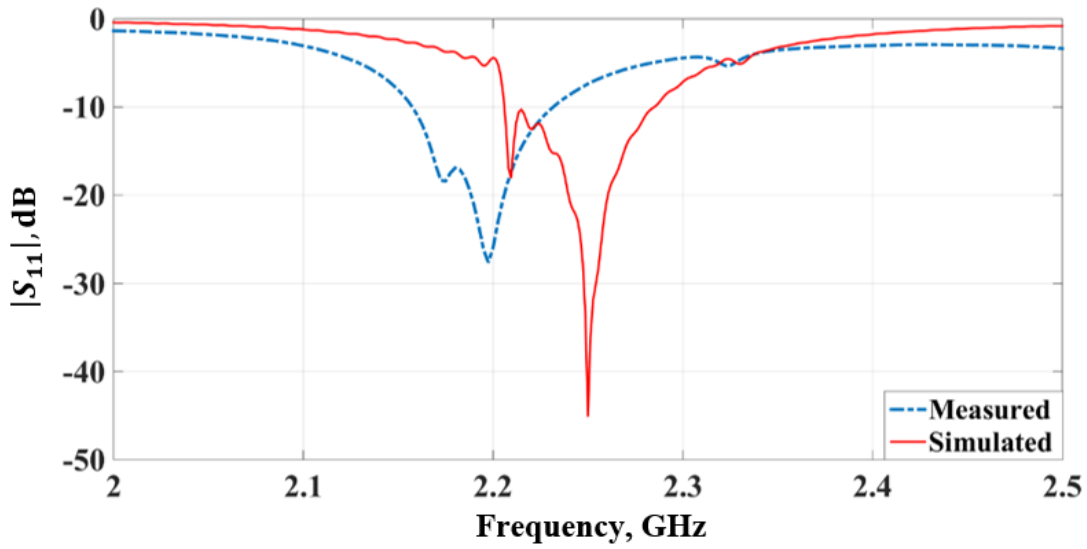

Figure 42 S_{11} and bandwidth of the modified B-SFRSA

This difference may arise from the thin dielectric sheet used to integration of two layers. In spite of a slight frequency shift bandwidth of the produced antenna, 73 MHz, satisfy the desired requirements. In order to excite the antenna in the desired frequency value (2.25 GHz), some modifications can be easily done. Besides, it should be indicated that when the antenna layers are tightly integrated to each other using press machine, loss observed in SFSA is reduced. Furthermore, to remove the

deficiencies due to electroplating through-hole process, via holes are manually soldered after the press operation.

In order to compare patterns of the simulated and fabricated antenna, far-field patterns of the produced antenna are measured. These measurement results are given in Figure 44. Details of the measurement setup can be also seen in Figure 43 in comparison with simulated patterns.

(a)

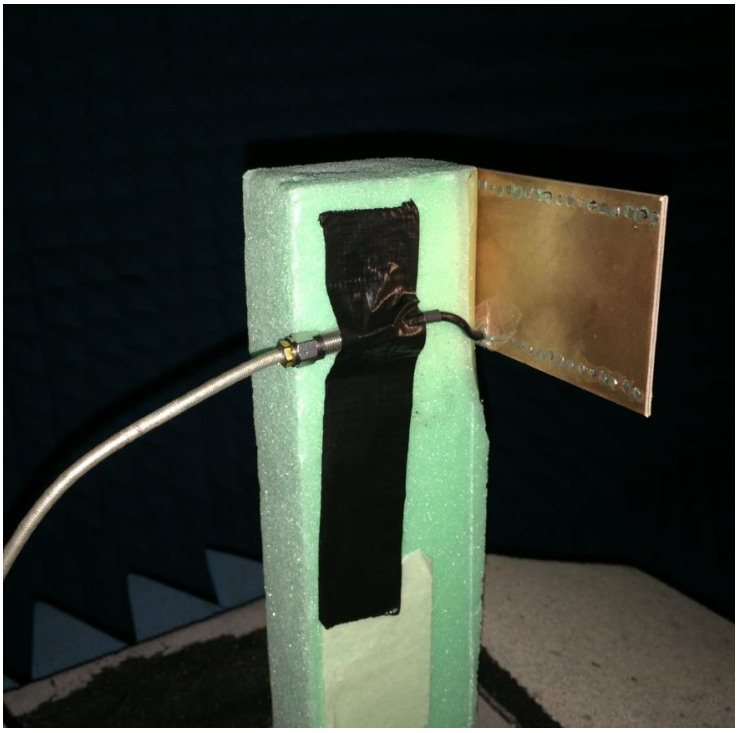

(b)

Figure 43 View of the measurement setup:

(a) front , (b) back

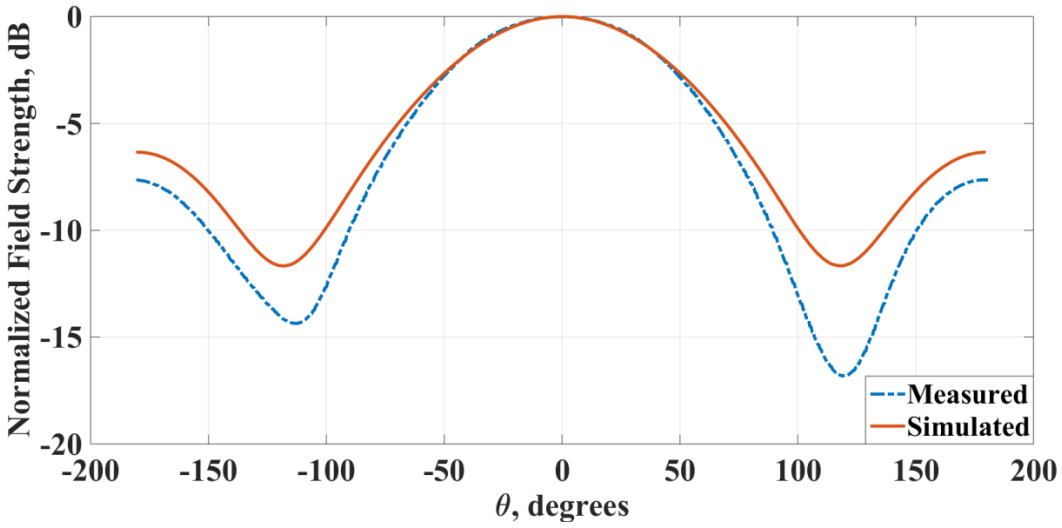

(a)

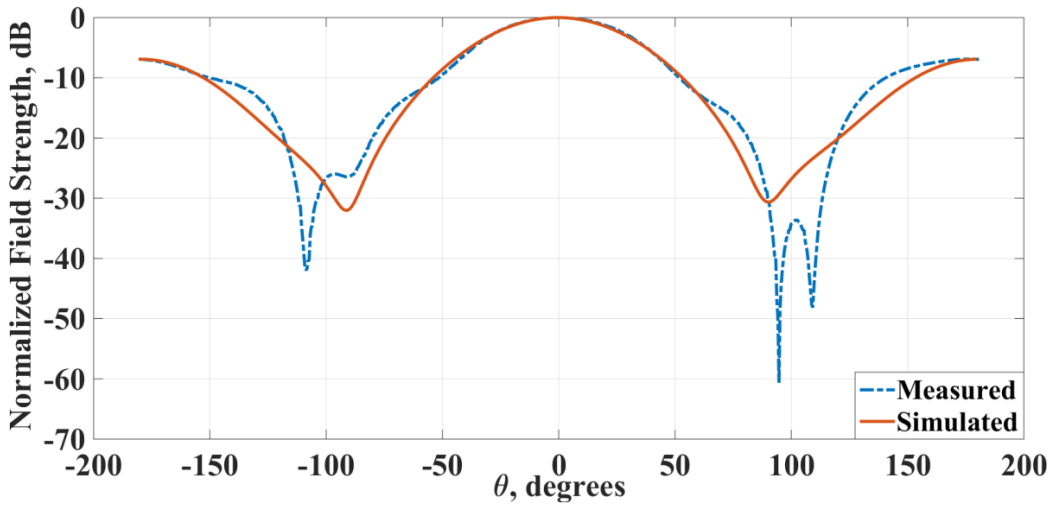

(b)

Figure 44 Normalized radiation patterns obtained by simulations and measurements B-SFRSA: (a) E-plane, (b) H-plane

Figure 44 shows that simulation and measurement results are compatible with each other. However, some deviations are also appeared in the measurement results. These differences may occur due to measurement set-up. Furthermore, connectors are not included in the simulations.

Designed and fabricated antenna includes a transverse stub to obtain a wider bandwidth. It is expected that this feed stub causes high cross-polarization at principal planes. Thus, cross-polarizations at the E- and H- planes are also measured. Differences between the measured co- and cross-polarized fields are 12 and 25 dB in H and E planes. Cross-polarization at H-plane is more dominant respect to the one in E-plane since the stub is placed along the slot.

As mentioned in the introduction section, the main objectives of this thesis is fabricating an array antenna that can be wrapped around a metallic cylinder. B-SFRSA is used in this array since it satisfies the given requirements. Details about the design and production process of array are explained in Chapter 4.

CHAPTER 4

DESIGN, FABRICATION AND MEASUREMENT OF A CYLINDRICAL ARRAY OF STRIPLINE FED SLOT ANTENNAS

Development of a stripline fed slot antenna element that can be used in a cylindrical array is explained in detail in previous chapters. It is demonstrated that B-SFRSA satisfies the design requirements. Thus, a cylindrical antenna array with feed network is designed using this antenna. Design, fabrication and measurement of this conformal antenna array is explained in sections 4.1 and 4.2.

4.1 Design of the Cylindrical Antenna Array

Antenna array consisting of two B-SFRSA elements and feed network is designed to be wrapped around a metallic surface of radius. First, an array is designed as a planar array. Then, it is wrapped around a cylinder and simulated. Designed planar array is modelled in CST as in the Figure 45 and Figure 46.

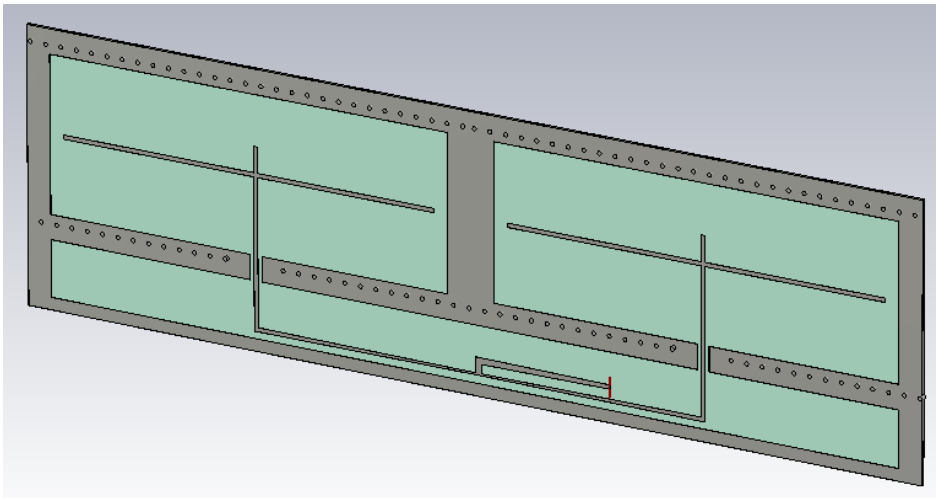

Figure 45 View of the designed array feed section

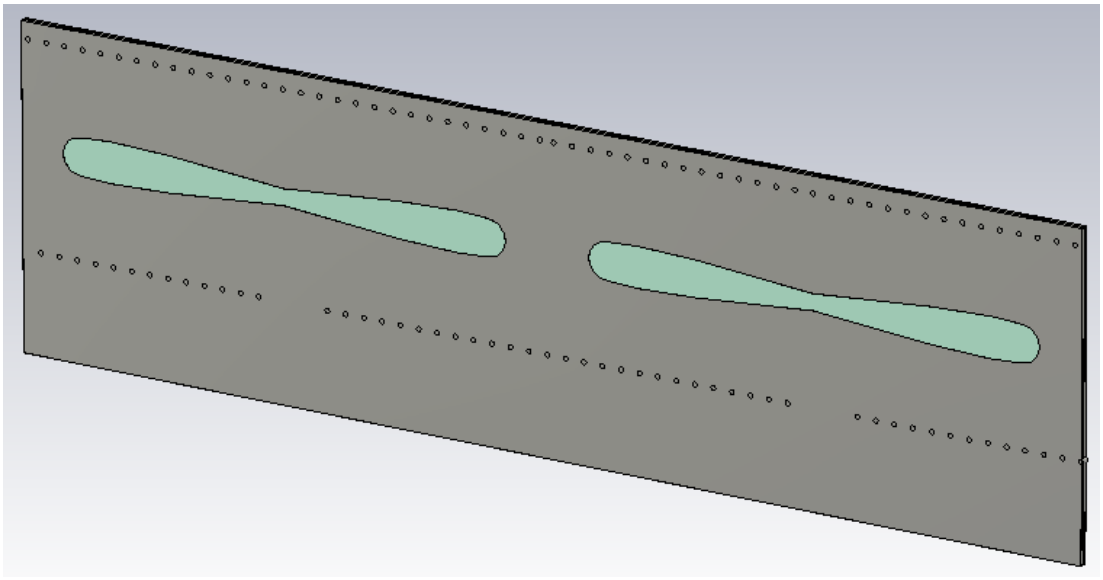

Figure 46 View of the designed array

Results of the S_{11} simulations performed for planar array is given in Figure 47.

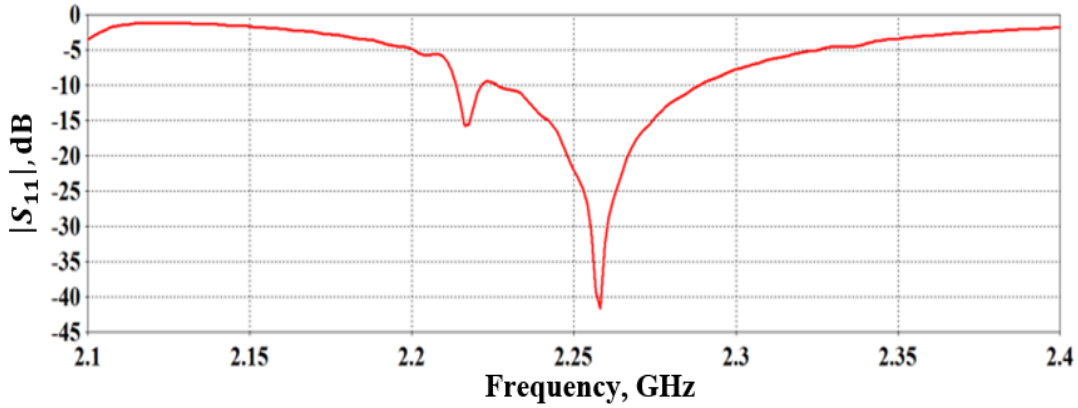

Figure 47 S_{11} and bandwidth of the conformal array

Return loss of the designed array is greater than 41 dB at 2.26 GHz and bandwidth of the array is nearly 77 MHz. These results comply with the performance of B-SFRSA given in section 3.3. Designed feed network can be seen in Figure 45. This network is used to transform 50 ohm antenna input impedance to 50 ohm single port feed impedance. In order to achieve this, 50 ohm antenna input impedance is firstly transformed to 70 ohm then, this 70 ohm is again transformed to 50 ohm feed input impedance. Schematic details of the feed network are given in Figure 48.

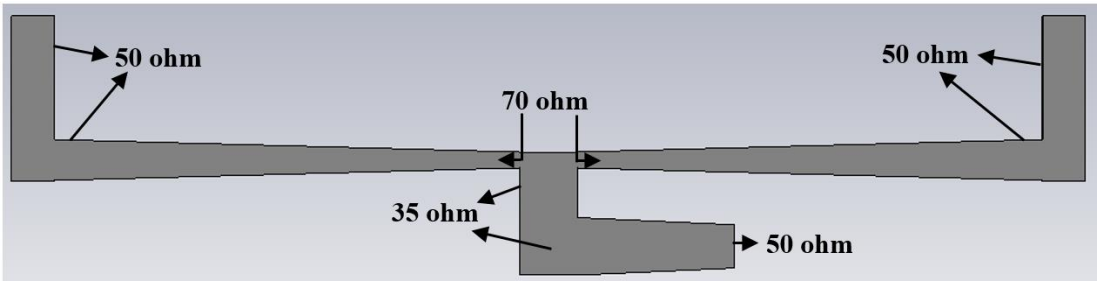

Figure 48 Feed network of the array

It is seen that tapered line is used to match 70 Ω to 50 Ω in Figure 48. A feed network with quarter-wave transformer section instead of tapered line is also designed. The S_{11} values obtained by these two feed networks are compared in Figure 49.

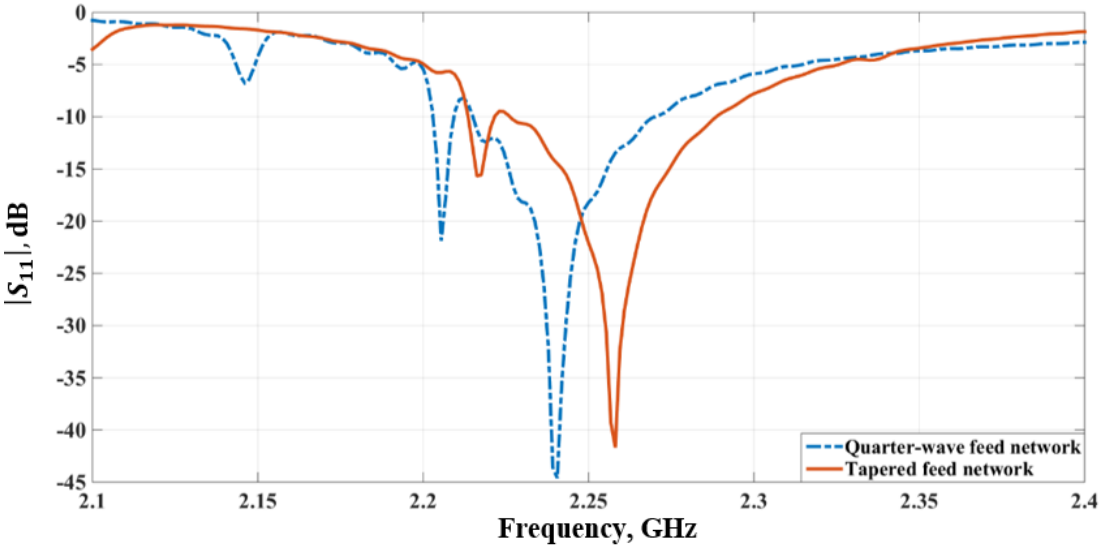

Figure 49 Comparison between S_{11} values obtained by a feed network with quarter-wave transformer and by a feed network with tapered line

Figure 49 shows that similar results are obtained from two feed networks. However, bandwidth of the antenna is approximately 68 MHz for quarter-wave feed network and 77 MHz for tapered feed network. Thus, it is decided to use tapered feed network at the conformal (cylindrical) antenna design.

After completing the planar array design, array parameter are optimized for the cylindrical array. Cylindrical array is modelled and simulated by CST Microwave Studio. Although all simulations, up to now, are performed by using the Transient Solver® of CST, Frequency Solver is used for cylindrical array. For non-planar geometries, Transient Solver® does not support waveguide port structure which is the most used port type for the stripline feed structures. However, Frequency Solver, supports the waveguide port structure for conformal geometries. Return loss of the array and far-field radiation patterns can be easily calculated by Frequency Solver. There are some differences between the results obtained by two solvers due to their numerical approaches. Transient Solver® solves problems in time domain by using the Finite Integration Technique, on the other hand, Frequency Solver® solves problems in frequency domain by using the Finite Element Method. In order to show differences between two solvers, planar antenna array is simulated in both solvers and the S_{11} results are compared in Figure 50.

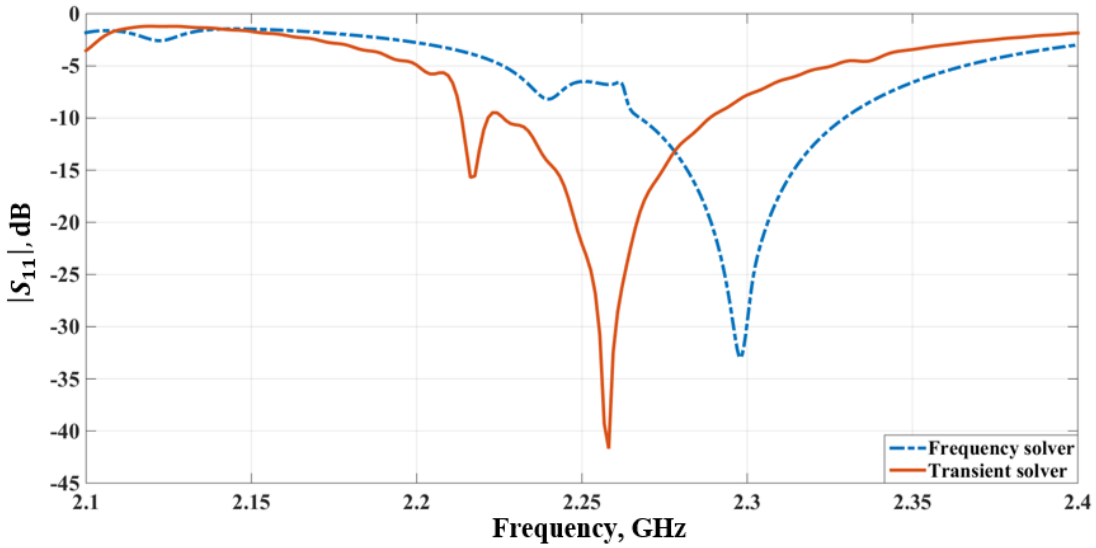

Figure 50 Comparison between the Frequency and Transient Solver

It is seen from Figure 50 that operating frequency is shifting towards upper frequency band in the Frequency Solver.

Cylindrical array shown in Figure 51 is simulated Frequency Solver of CST. Simulated S_{11} results for cylindrical array and planar array are compared in Figure 52. It is observed that input return loss performance of cylindrical array is very similar to planar case. There is a slight decrease in the frequency in case of cylindrical array.

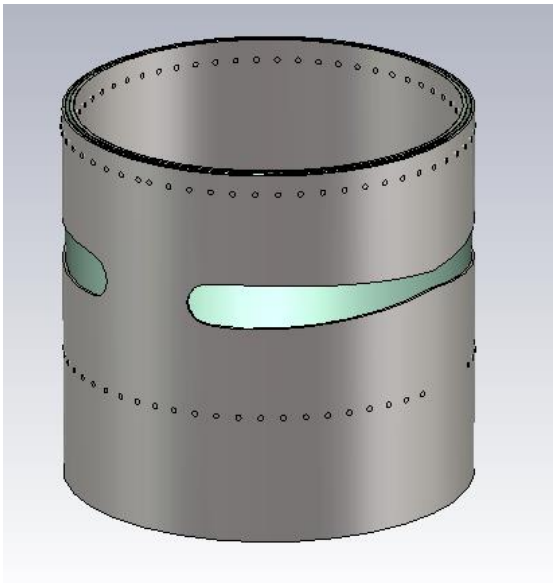

Figure 51 View of the designed conformal array

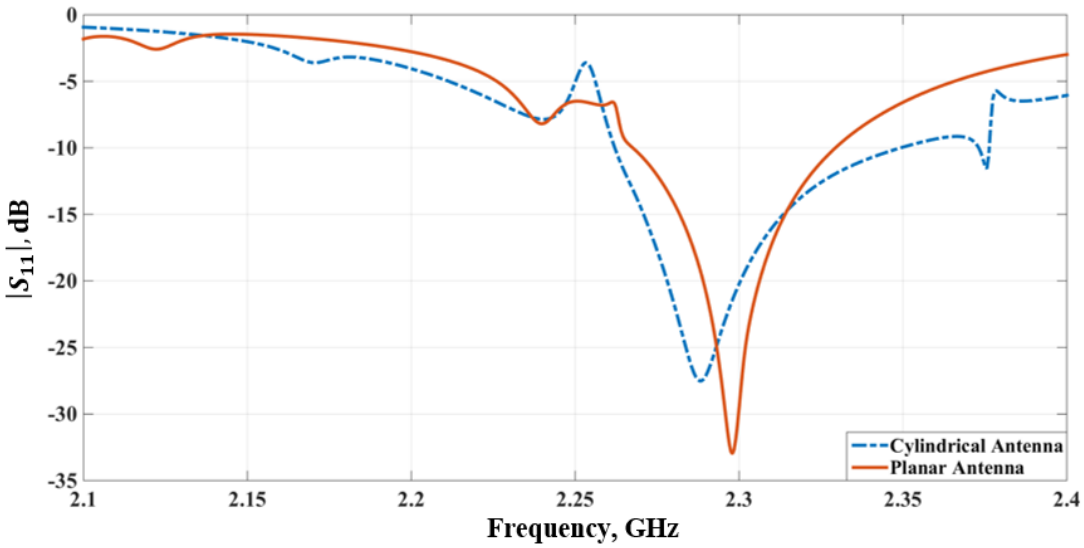

Figure 52 S_{11} results of the planar and cylindrical antenna

It is known from parametric studies performed in chapter 2 and 3 that operating frequency shifts to lower frequency when length of the slot is increased. Thus, this slight shift in the operating frequency is an expected result since length of the slot is increased during the bending process.

4.2 Fabrication and Measurement

In order to figure out whether the requirements given at Table 1 are met or not, designed antenna is fabricated. Fabrication process given in Chapter 3 is used to manufacture cylindrical antenna. First antenna is produced as a planar antenna, then it is bended by using a cylindrical body. However, due to cylindrical shape, vias are not electroplated. Two ground planes are electrically connected to each other by soldering through vias. The photograph of the fabricated antenna is given in Figure 53.

Figure 53 Fabricated cylindrical antenna

The input return loss characteristics obtained by measurements are given in Figure 54 in comparison with results for planar array.

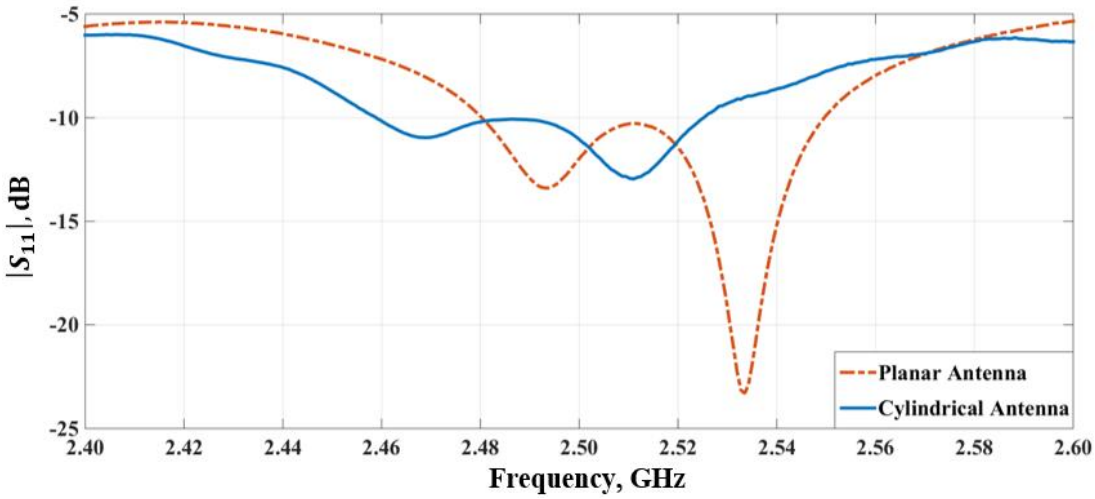

Figure 54 Fabricated planar and conformal array S_{11} result

Bandwidths of the planar and cylindrical antenna are 70 MHz and 66 MHz, respectively. These values satisfy the bandwidth requirement given in Table 1 but some unexpected results are occurred during the integration process. Operation frequency shifts toward upper frequency band with respect to designed antenna result given in Figure 47. Figure also shows that amplitude of S_{11} is decreased after the bending operation. As explained at the section 3.3, a thin dielectric sheet (prepreg) is used to integrate the layers. Thickness and amount of this prepreg are effecting position of the operation frequency. During the bending, dimensions of the slot and stripline feed can be changed independently. This cause an impedance mismatch between the slot and stripline feed. Furthermore, slot length is slightly increased during bending. This results in a slightly decrease in the operating frequency.

Far field patterns of the cylindrical antenna in roll plane is measured and presented in Figure 55.

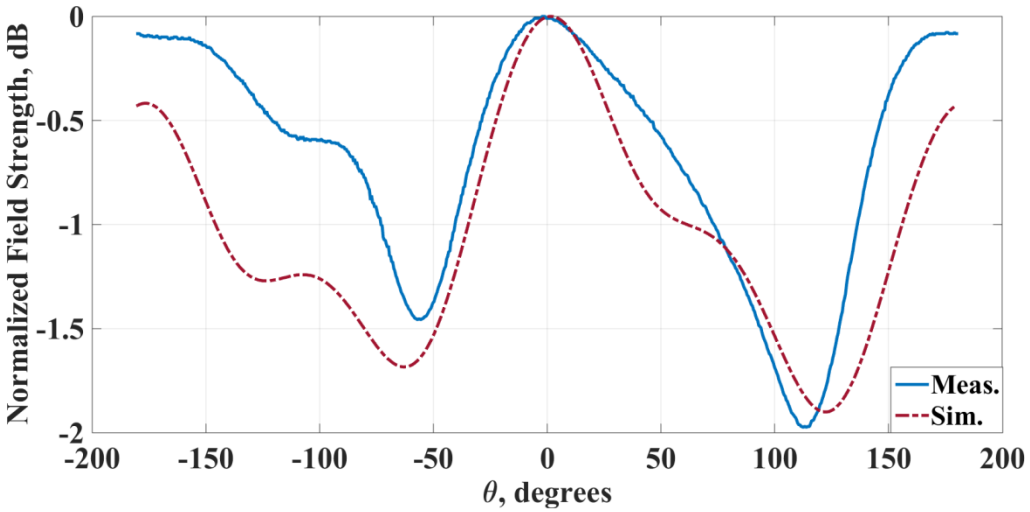

Figure 55 Comparison of normalized of radiation patterns obtained by simulations and measurements in the roll plane

Figure 55 shows that the pattern is omni-directional and fluctuations are in ± 1 dB. Furthermore, it should be noticed that there are approximately 0.3 dB differences between the measured and simulated results when theta is equal to ±180 degree. It is due to the fact that, cylindrical conformal antenna could not be placed on a cylindrical body at the pattern measurement process. Thus, ending and starting points of the antenna could not be exactly faced to each other, so that there is a slight gap between these points. However, this is an acceptable result since max. and min. value of the received signal amplitude still remains in ± 1 dB limit.

CHAPTER 5

DESIGN, FABRICATION AND MEASUREMENT OF A COPLANAR PATCH ANTENNA

Stripline fed slot antennas are deeply investigated in preceding chapters. However, since these antennas consists of two layers, integration of these two layer for cylindrical case causes some so degradations in their radiation characteristics. To overcome these problems more advanced fabrication tools and techniques are required which may increase the production cost. Therefore, an alternative antenna of a single layer is designed and fabricated. Coplanar patch antenna is a good candidate. In this chapter, design, fabrication and measurement results of the coplanar patch antenna fed by coplanar waveguide are explained. Design of the antenna and related parametric study are given in section 5.1. Designed antenna is fabricated and measured. Fabrication and measurement results are given in 5.2.

5.1 Design of the Coplanar Patch Antenna

The geometry of the coplanar patch antenna is shown in Figure 56. Coplanar patch antenna, called CPA, consists of a microstrip patch antenna and ground conductor which is closely placed around the microstrip patch. Geometrical structure of the CPA is similar to slot loop antenna. Appropriate feed structure for this antenna is grounded coplanar waveguide (GCPW).

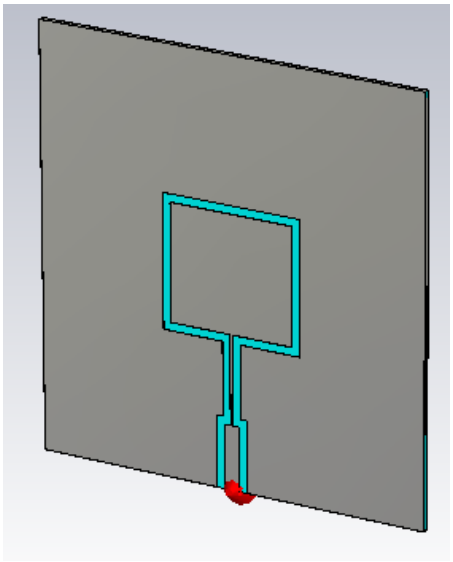

Figure 56 View of the CPA

Antenna is designed by considering the requirements given at Table 1. First, a microstrip patch antenna shown in Figure 57 is designed by using formulas given in [18].

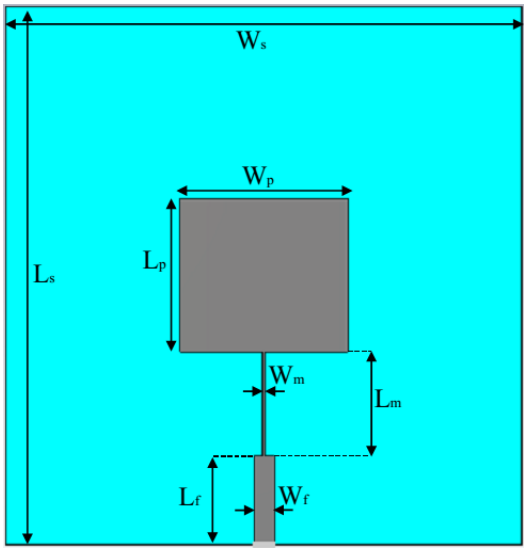

Figure 57 Designed microstrip patch antenna

Dimensions of the designed patch antenna are given in Table 8.

Table 8 Parameters of the Microstrip Patch Antenna

Parameters	Description	Values (mm)
t_c	Thickness of conductor	0.133
t_s	Thickness of substrate	1.52
W_s	Width of substrate	121.5
L_s	Length of substrate	126.8
W_f	Width of feed	4.7
L_f	Length of feed	21
W_m	Width of match	0.8
L_m	Length of match	24.4
W_p	Width of patch	39.5
L_p	Length of patch	36

Input return loss characteristic of the designed patch antenna is given in Figure 58.

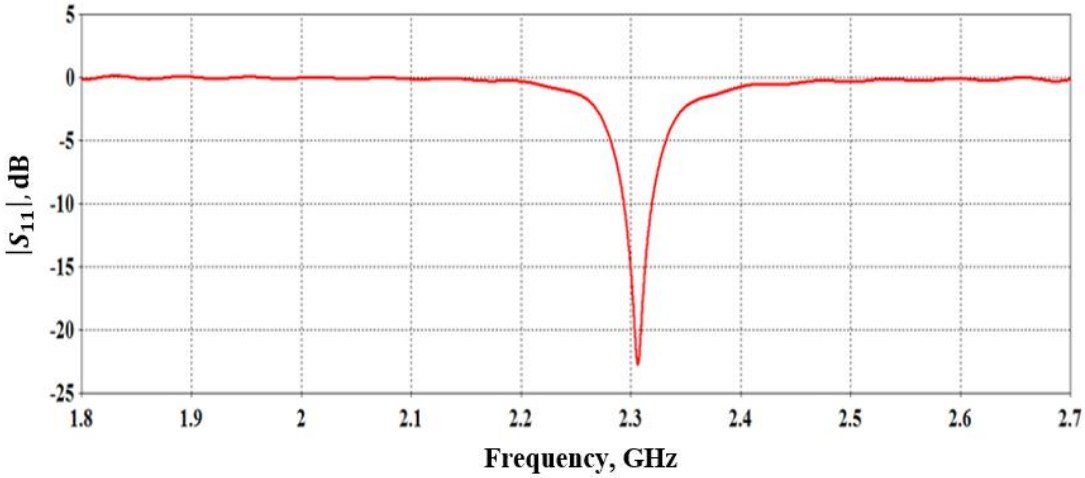

Figure 58 S_{11} of the microstrip patch antenna

Bandwidth and S_{11} of the antenna is found 26 MHz and -23 dB, respectively. After obtaining this result, CPA is designed by placing a ground conductor around and leaving a space (*S*) between the ground plane and microstrip patch antenna. View of the CPA and simulation result are given in Figure 59 and Figure 60, respectively.

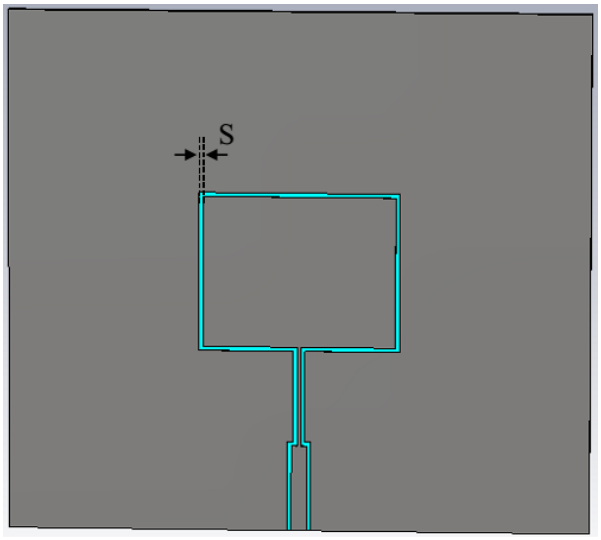

Figure 59 Designed CPA

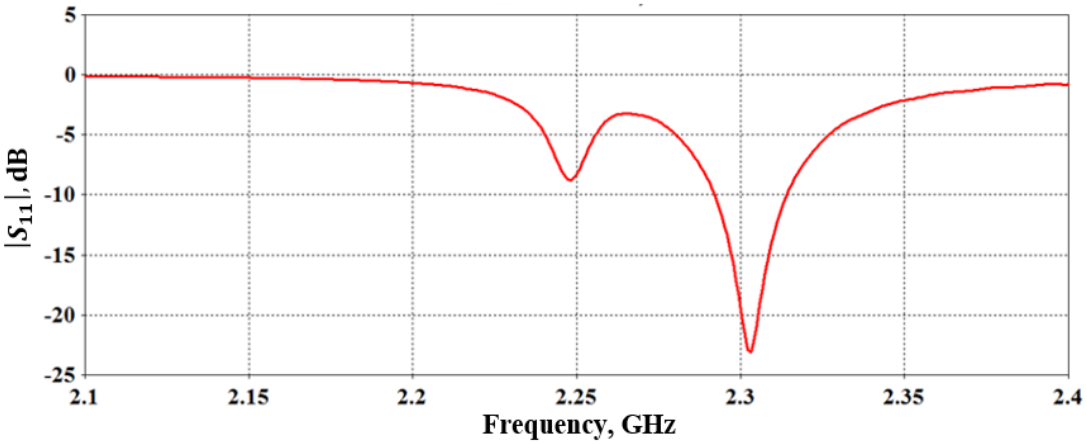

Figure 60 S_{11} of the CPA for S=1 mm

It is seen from Figure 60 that a second resonance is occurred at the 2.25 GHz. This second resonance point is caused by coplanar structure. It is shown in [19] that second resonance can be easily controlled by addition of parasitic elements to the structure.

To obtain a wider bandwidth the slots are added to the left and right parts of the loop in a parallel configuration as shown in Figure 61. By gaining experience through

parametric study, modified CPA (U-CPA) is designed. Dimensions are given in Table 9. The substrate material is Rogers 3003.

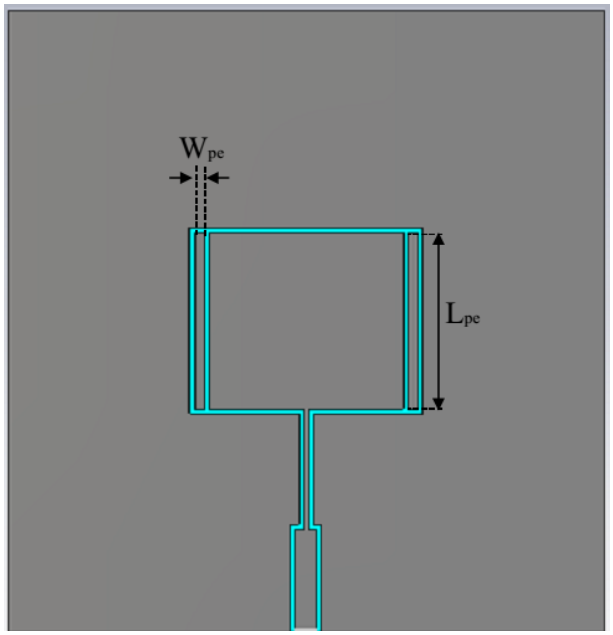

Figure 61 Updated design of the CPA (U-CPA)

Table 9 Parameters of the U-CPA

Parameters	**Description**	**Values (mm)**
t_c	Thickness of conductor	0.133
t_s	Thickness of substrate	1.52
S	Slot width	3.25
W_s	Width of substrate	121.5
L_s	Length of substrate	126.8
W_f	Width of feed	4.4
L_f	Length of feed	21
W_m	Width of match	0.8
L_m	Length of match	24.4
W_p	Width of patch	39.5
L_p	Length of patch	36

W_{pe}	Width of parasitic elements	1.25
L_{pe}	Length of parasitic elements	36

According to these parameters, input return loss characteristic of the designed U-CPA is given in Figure 62.

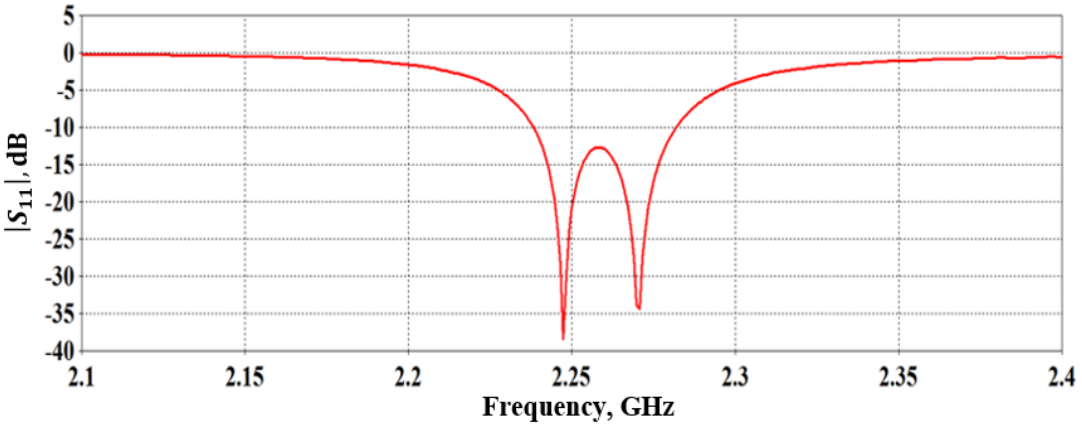

Figure 62 S_{11} and bandwidth of the U-CPA

Figure 62 shows that 10 dB and bandwidth of the antenna is approximately 45 MHz. To understand the effects of the parameters of U-CPA on radiation performance study is performed.

1. Effects of width of the parasitic elements, W_{pe}

First parametric study is performed for width of the parasitic elements. Simulations of U-CPA are repeated for three different values of W_{pe}. Obtained input return loss values are plotted in Figure 63.

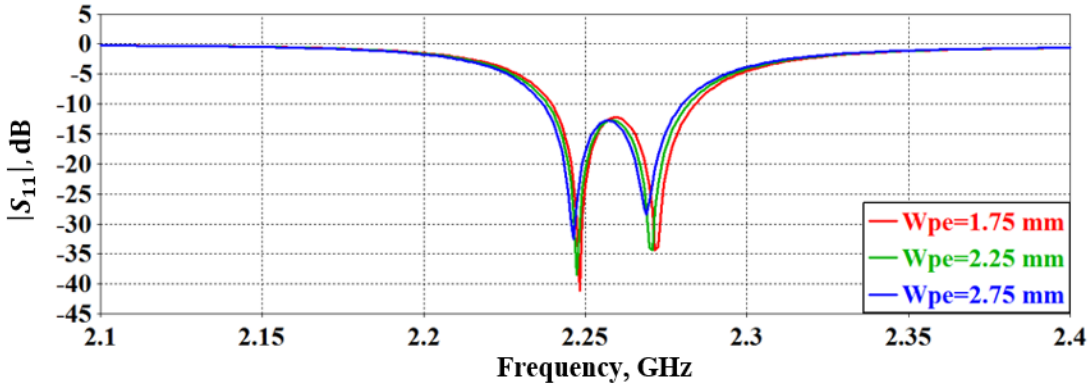

Figure 63 S_{11} of the U-CPA with respect to W_{pe}

Figure 63 shows that changes in W_{pe}.does not affect the operating frequency band significantly. Width of the parasitic elements influences the amplitude of the S_{11}. It is an expected result since this antenna behaves as a microstrip patch antenna [5]. It is known that change in width of the microstrip antenna also cause a change in amplitude of the return loss. Same situation is valid for the parasitic elements, as well.

2. Effects of length of the parasitic elements, L_{pe}

Another parametric simulation is carried out for the length of the parasitic element. Results of the simulations are given in Figure 64, for different L_{pe} values.

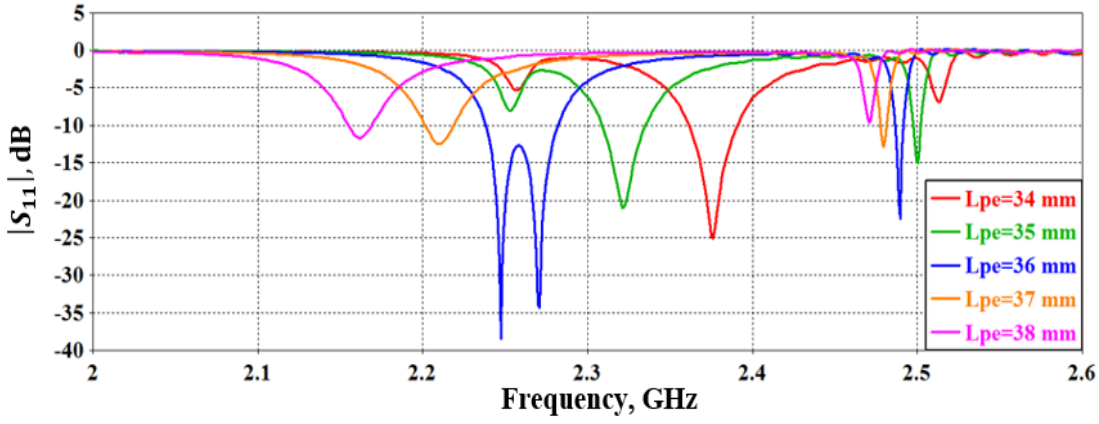

Figure 64 S_{11} of the U-CPA with respect to L_{pe}

It can be easily seen from figure that length of the parasitic elements has important effect on S_{11}. As indicated at the first parametric study, CPA or U-CPA behaves like a microstrip antenna. It is known that length of the microstrip antenna determines center of the operating frequency. This rule is also valid for the parasitic elements since they are radiating patches. Thus, operation frequency shifts when L_{pe} (also L_p) is changed.

3. Effects of the slot width, *S*

Last parametric calculation is performed for slot width which is a gap between the ground plane and patch antenna. S_{11} results are given in Figure 65, for different S values.

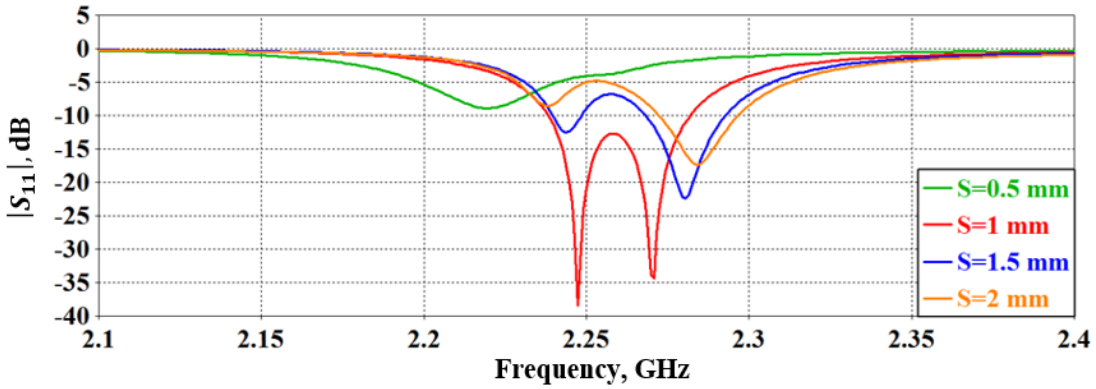

Figure 65 S_{11} of the U-CPA with respect to S

Figure shows that slot width dramatically affects return loss of the antenna. Changes in the slot width are affecting the second resonance of the antenna. Second resonance is disappeared when S gets small values. Even the resonance characteristic disappears if S is too small. Besides, broadband bandwidth characteristic becomes dual band behavior when the slot width is increased. Thus, S value should be chosen carefully.

5.2 Fabrication and Measurement

Fabrication process of the antenna is relatively easy compared to SFSAs since it consists of a single layer, and there are no vias which require electroplating. The photograph of the fabricated antenna is given in Figure 66.

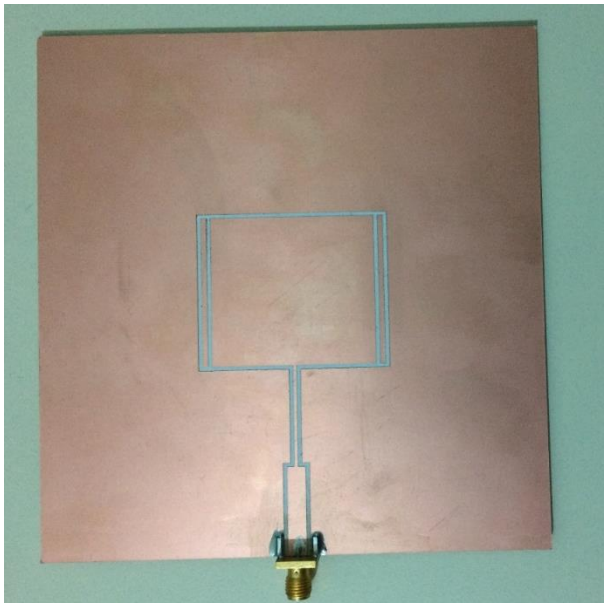

Figure 66 Fabricated U-CPA

Measurement and simulation results of S_{11} are given in Figure 67.

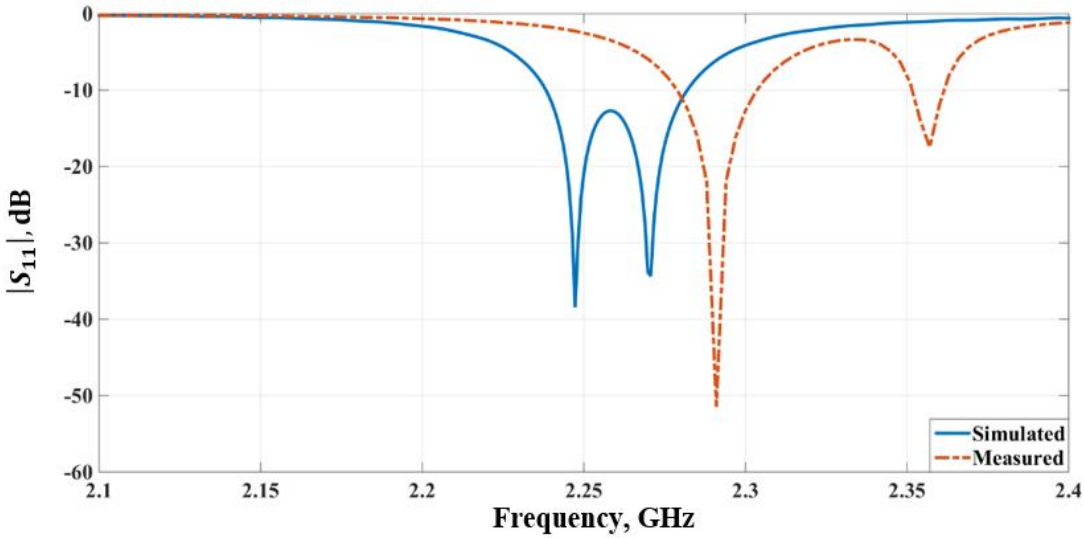

Figure 67 S_{11} results of the measured and simulated U-CPA

It is observed that measured and simulated input return loss characteristics are different than each other. There is an approximately 70 MHz shift in operating frequency band. To understand the reason of this difference, SMA connector is included in the simulation, as shown in Figure 68. Return loss characteristics by simulations of antenna with connector are given in Figure 69.

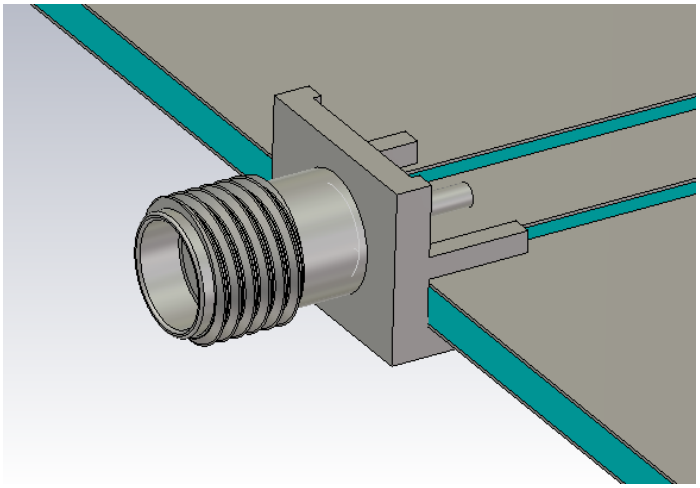

Figure 68 Added SMA connector

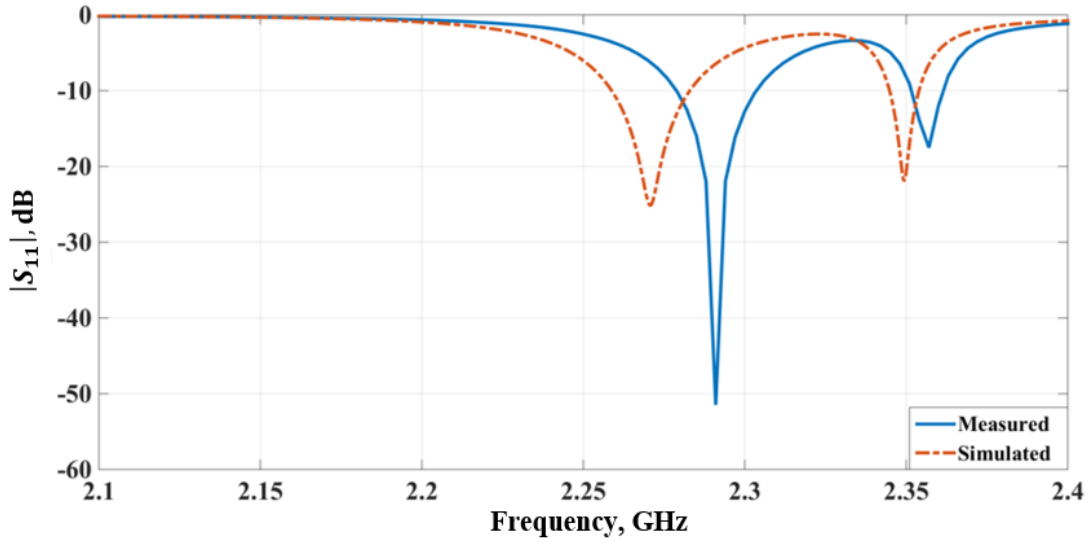

Figure 69 S_{11} and bandwidth of the U-CPA with SMA connector

It is observed that measured and simulated results are in a better agreement.

In addition the return loss measurement, antenna far-filed patterns are also measured. Measured patterns are compared with simulated results in Figure 70.

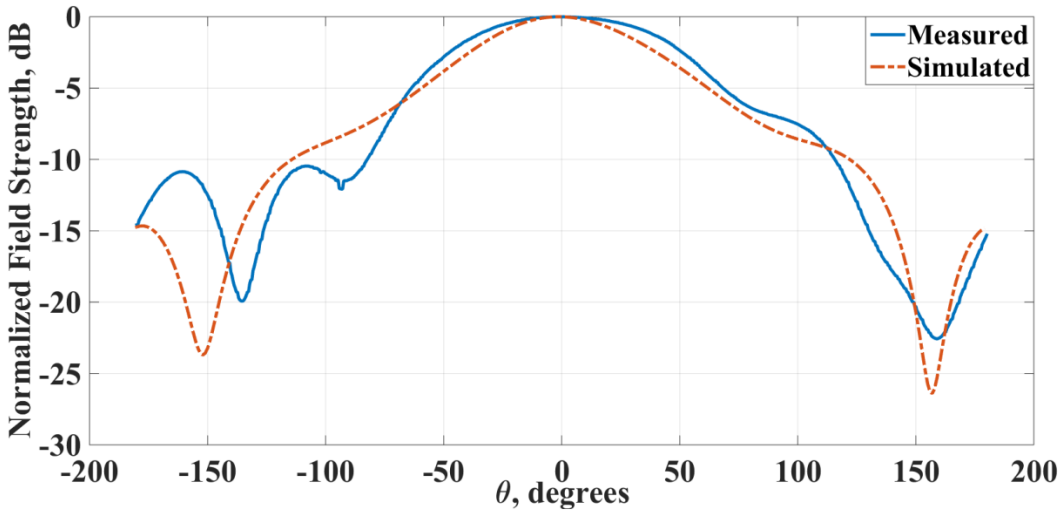

(a)

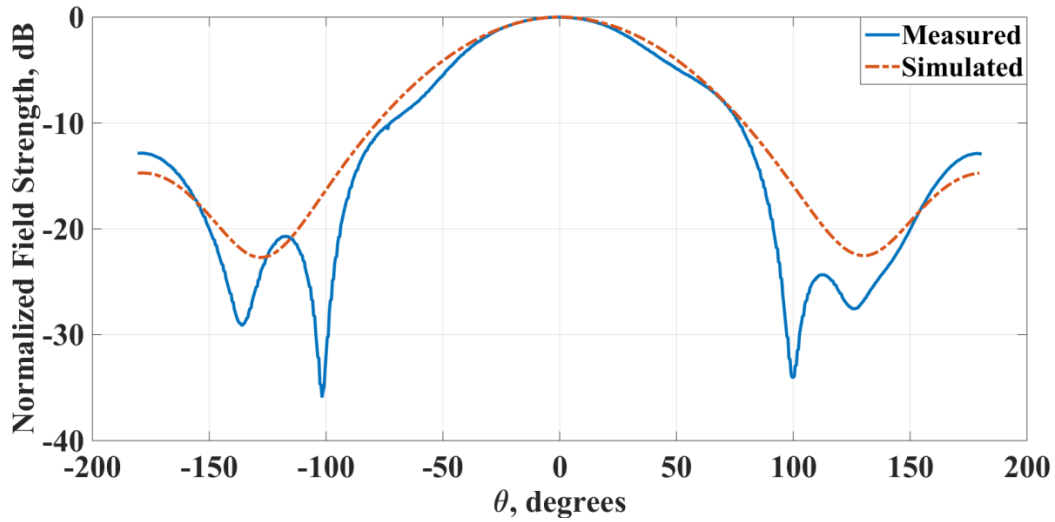

(b)

Figure 70 Normalized co-polar radiation patterns of the simulated and fabricated U-CPA: (a) E-plane, (b) H-plane

It is observed that measured and simulated pattern agree well with each other. Cross-polarized fields at the E- and H-planes are also measured. Differences between the measured co- and cross-polarized fields at the H- and E-planes are found as 8 dB and 17 dB, respectively. This results show that cross-polarization in the H plane is more dominant.

Fabricated antenna measurement results show that the bandwidth requirement is not satisfied. Although fabrication process is easier than stripline fed slot antennas, array of this antenna element will not satisfy the requirements of telemetry application.

CHAPTER 6

CONCLUSIONS

The main objective of this thesis is to design a cylindrical array for telemetry applications. This array should have an omni-directional pattern in azimuth (roll plane) in frequency band of 2225-2275 MHz. First, as array elements, stripline fed slot antennas and a coplanar patch antenna are investigated, fabricated and measured. The first designed simple stripline fed rectangular slot antenna has a bandwidth of 45 MHz. Since this antenna does not satisfy the required bandwidth, slot structure is modified. Final stripline fed slot antenna has a rounded bow-tie slot and a transverse stub is added to the offset stripline. It is shown that bandwidth of the fabricated antenna is 70 MHZ which satisfies the requirements. Thus a two element array of B-SFSRA with an appropriate feed network is designed. After bending the antenna around a cylindrical body, bandwidth becomes 66 MHz and still satisfies the requirement. It is observed that input return loss characteristics of the planar antenna and cylindrical antenna are similar to each other. It should be noticed that antenna operating frequency shifts towards the lower frequency band slightly when the planar antenna is wrapped around a cylindrical body. There are also some differences in the simulated and measured return loss characteristics even in planar antenna case. These are due to imperfections in the fabrication process. First of all to assemble two layers of the antenna, a prepreg, thin dielectric sheet is put between two layers in the press machine. Thus inclusion of prepereg material in the simulations can result in a better agreement between simulations and measurements. As an alternative fabrication method, rivets can be used for integration and electrical connection between the ground planes. This method will take less time to integrate the layers and it is a very simple operation compared to the press process. Moreover, if rivets are used, there is

no need for electroplating of vias which also causes deviations in the characteristics. Electrical conductivity can be ensured since the rivets are made of copper.

Radiation patterns of the fabricated cylindrical array antenna in the roll plane are measured in the anechoic chamber of METU EEE Department. It is seen that omni-directional patterns are obtained. Fluctuations of omni-directional pattern is in ±1 dB range which proves that the fabricated antenna has very good omni- directional radiation characteristic.

As an alternative for the stripline fed slot antennas, a coplanar patch antenna is designed and fabricated, as well. However, CPA could not satisfy the bandwidth requirement. Its bandwidth is approximately 30 MHz.

In this thesis, conformal cylindrical antenna array is designed, fabricated and measured. As a conclusion, it can be said that the designed cylindrical antenna satisfies all design requirements. However, to improve the radiation characteristics of the antenna, better fabrication techniques should be developed.

As a future work, innovative and novel antenna topologies that can be easily fabricated and provide better radiation characteristics, such as wider bandwidth, can be investigated for cylindrical arrays required in avionics applications.

REFERENCES

[1] Jayakumar, I.; Garg, Ramesh; Sarap, B.; Lal, B., "A conformal cylindrical microstrip array for producing omnidirectional radiation pattern," *Antennas and Propagation, IEEE Transactions on*, vol.34, no.10, pp.1258, 1261, Oct 1986.

[2] Post, R.; Stephenson, D.T., "The design of a microstrip antenna array for a UHF space telemetry link," *Antennas and Propagation, IEEE Transactions on*, vol.29, no.1, pp.129, 134, Jan 1981.

[3] Zentner, R.; Sipus, Z.; Herscovici, N.; Bartolic, J., "Omnidirectional stacked patch antenna printed on circular cylindrical structure," *Antennas and Propagation Society International Symposium, 2002. IEEE*, vol.2, no., pp.272, 275 vol.2, 2002.

[4] Qiu Jinghui; Zhong Lingling; Du Hailong; Li Wei, "Analysis and simulation of cylindrical conformal omnidirectional antenna," *Microwave Conference Proceedings, 2005. APMC 2005. Asia-Pacific Conference Proceedings*, vol.4, no., pp.4, 4-7 Dec. 2005.

[5] Herscovici, N.; Sipus, Z.; Kildal, P.-S., "The cylindrical omnidirectional patch antenna," *Antennas and Propagation, IEEE Transactions on*, vol.49, no.12, pp.1746, 1753, Dec 2001.

[6] Löcker, C.; Vaupel, T.; Eibert, T.F., "Radiation Efficient Unidirectional Low-Profile Slot Antenna Elements for X-Band Application," *Antennas and Propagation, IEEE Transactions on*, vol. 53, no.8, pp. 2765, 2768, Aug. 2005.

[7] del Carmen Raola, M., "Analysis of Conformal Antennas for Avionics Applications," M.Sc. Thesis, Chalmers University of Technology, Gothenburg, Sweden, 2007.

[8] Fischer, A. C., "Conformal Microstrip GPS Antenna for Missile Application," M.Sc. Thesis, California Polytechnic State University, San Luis Obispo, USA, 2011.

[9] Chen, C.; McKinzie, W.E.; Alexopoulos, N.G., "Stripline-fed arbitrarily shaped printed-aperture antennas," *Antennas and Propagation, IEEE Transactions on* , vol.45, no.7, pp.1186, 1198, Jul 1997.

[10] Li, K.; Cheng, C.H.; Matsui, T.; Izutsu, M., "Coplanar patch antennas: principle, simulation and experiment," *Antennas and Propagation Society International Symposium, 2001. IEEE*, vol.3, no., pp.402, 405 vol.3, 8-13 July 2001.

[11] Horan, S., "Introduction to PCM Telemetering Systems," CRC Press, United States of America, 1993.

[12] Data Sheet, *RO3000® Series Circuit Materials High Frequency Laminates*, ROGERS Corporation.

[13] IEEE Standard Test Procedures for Antennas," *ANSI/IEEE Std 149-1979*, vol., no., pp.0,1, 1979

[14] Kraus, John D., "Antennas Second Edition", Tata McGraw-Hill Editiıon, India, 1988.

[15] Dell, Brian C. "Transmission Line Design Handbook," Artech House, United States of America, 1991.

[16] Rosu I., "Microstrip Stripline and CPW Design," <http://www.qsl.net/va3iul>.

[17] Gheethan, A.A.; Anagnostou, D.E., "Broadband and Dual-Band Coplanar Folded-Slot Antennas (CFSAs) [Antenna Designer's Notebook]," *Antennas and Propagation Magazine, IEEE*, vol.53, no.1, pp.80, 89, Feb. 2011.

[18] Balanis, C. A., "Antenna Theory Analysis and Design Second Edition," John Wiley & Sons, United States of America, 1997.

[19] Tong, K.F.; Li, K.; Matsui, T.; Izutsu, M., "Wideband coplanar waveguide fed coplanar patch antenna," *Antennas and Propagation Society International Symposium, 2001. IEEE*, vol.3, no., pp.406, 409 vol.3, 8-13 July 2001.

APPENDIX

A. DESIGN OF A CYLINDRICAL PATCH ANTENNA

In this section, design procedure of a cylindrical antenna in CST is expressed by using the simple inset fed microstip patch antennas which is given at the Figure 71.

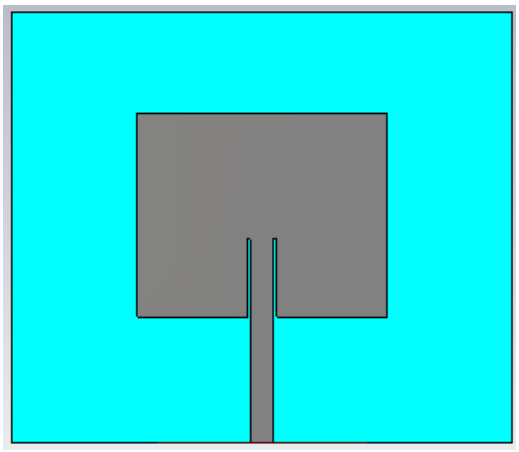

Figure 71 View of inset fed microstrip patch antenna.

In order to design a cylindrical shaped conformal antenna, substrate and ground plane can be removed from the design. New view of the antenna is given at Figure 72.

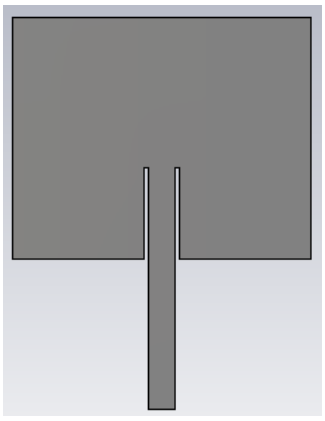

Figure 72 View of the antenna without the substrate and ground plane

Then, working coordinate system is set the middle of the lower fed edge as given at Figure 73

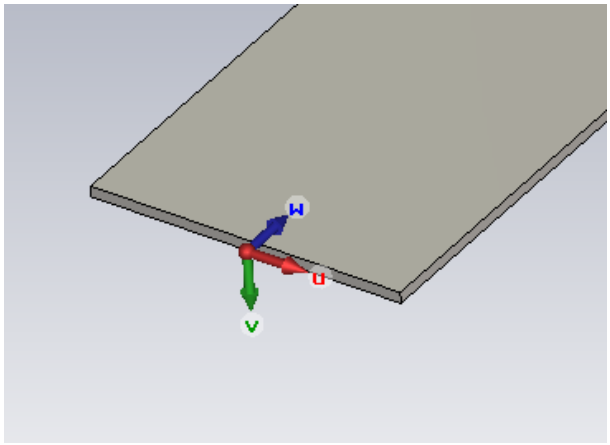

Figure 73 View of the local coordinate system in the fed edge

After setting the working coordinate system (WCS), radius of the desired cylindrical body can be adjusted as a parameter and WCS is moved to this distance as indicating at the Figure 74.

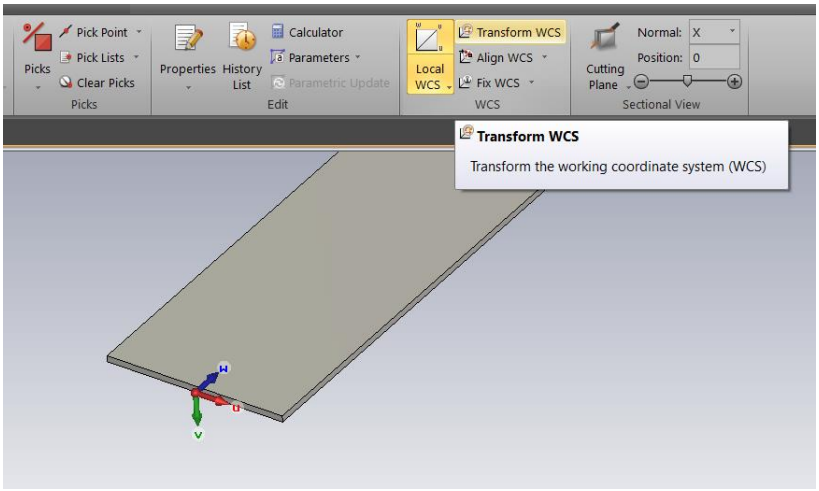

Figure 74 View of the WCS

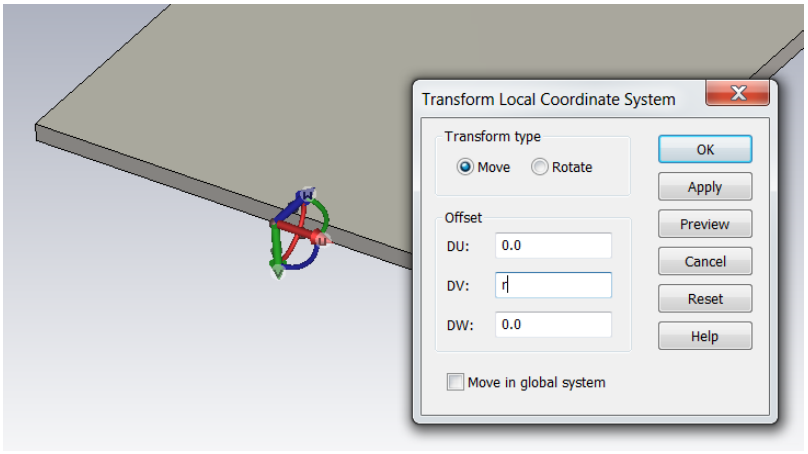

Figure 75 View of the WCS adjust menu

After defining the radius of the cylinder (r) as a parameter, it can be easily changed if the value of the radius is updated for the next studies. For instance, r can be set as 80 mm in this simulation. Then, we should define cylinder whose radius is 80 mm. Also, length and thickness of the cylinder can be adjusted as same with the substrate. Material of the substrate can be chosen as similar with the substrate, as well. View of the parameter definition of the cylinder is given at Figure 76.

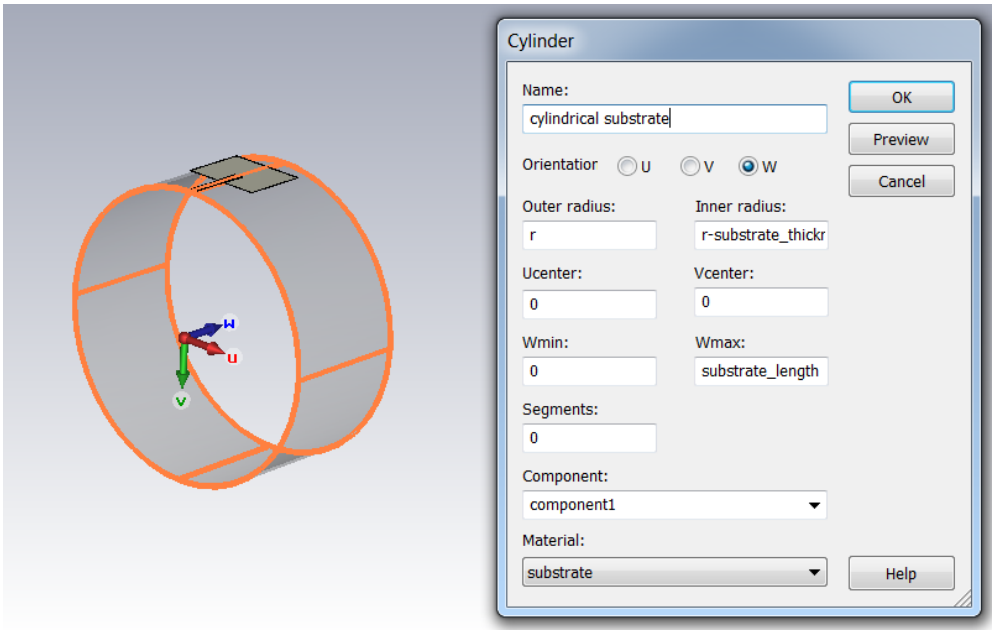

Figure 76 Definition of the cylindrical parameters

Now, patch element can be wrapped around the cylindrical body. In order to do it, patch element is firstly chosen in the navigation tree placed at the left side of the screen. Then, click the bend shape button in the software and click the cylindrical body twice to select it. After these operations, patch element and cylindrical body are adjusted for the bending operation. In order to bend the patch element, click the cylindrical body. Related screen shots are given in Figure 77, Figure 78 and Figure 79.

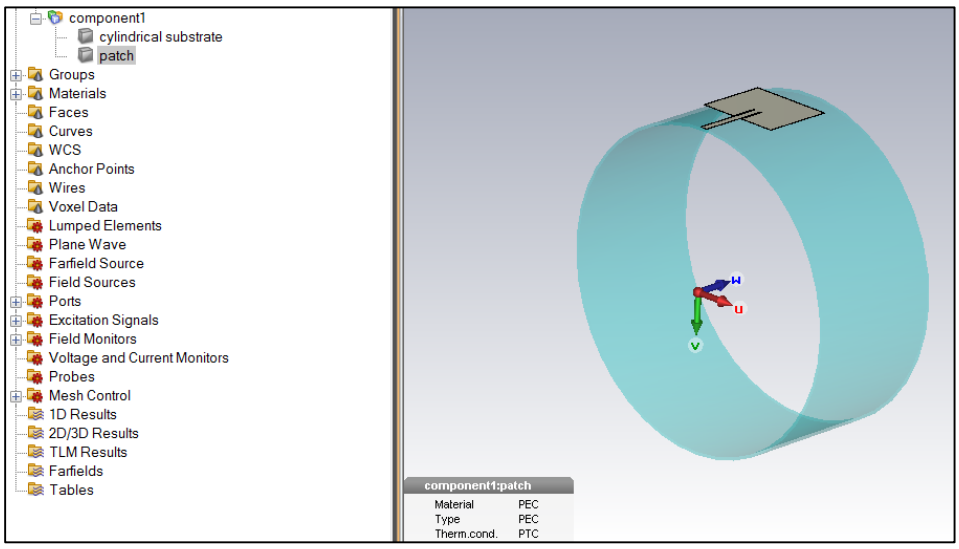

Figure 77 View of the patch element selection

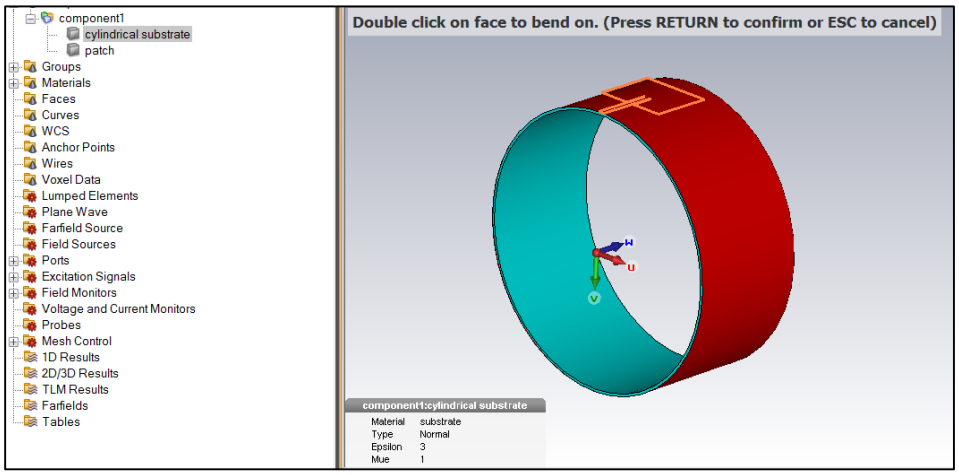

Figure 78 View of the bend face selection

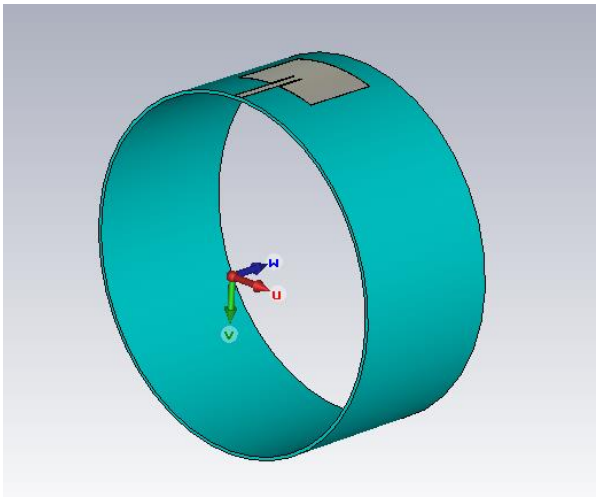

Figure 79 View of the rounded patch element

After the bending operation, patch element can be copied to obtain an antenna array. This operation can be easily achieved by using the transform button (rotation option) in the software. Number of patches and location angle of these antennas are easily configured as given at Figure 80 and Figure 81.

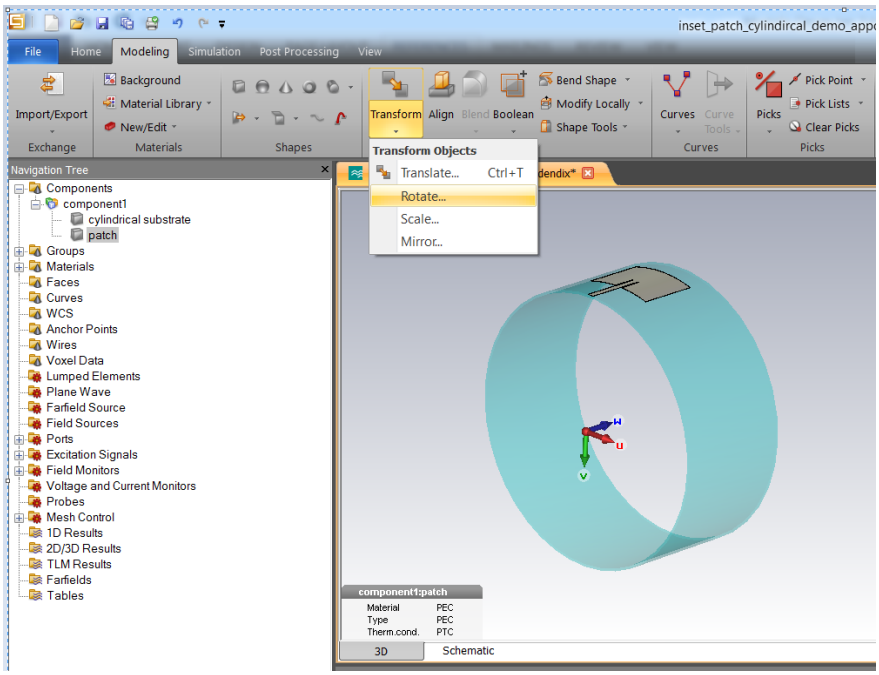

Figure 80 View of rotation operation

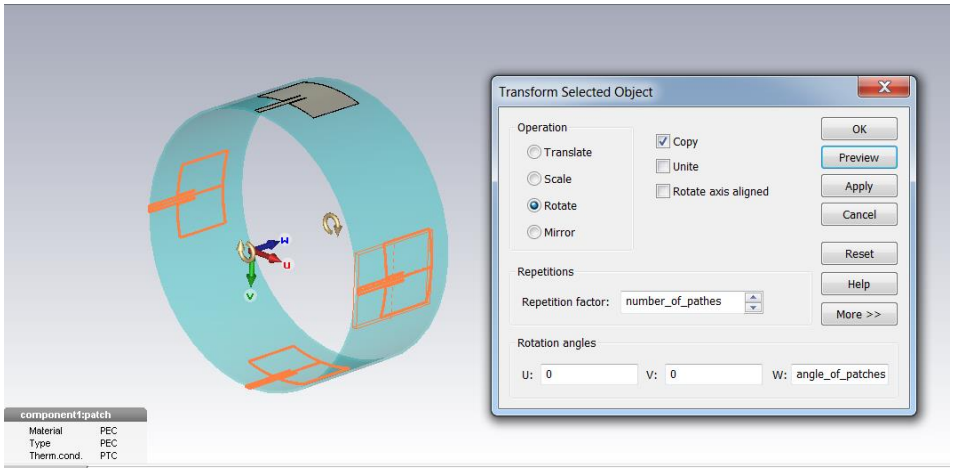

Figure 81 View of rotated patch elements

In the simulation example, number and angle of the patches are chosen 3 and 90°, respectively. After the patch element transformation, bottom ground plane of the antennas can be determined by using the extrusion button in the software. Thickness of the ground plane can be adjusted as same with the metal thickness in the design. However, inner surface of the substrate is firstly chosen for the extrusion operation. Related screen shots are given at the Figure 82, Figure 83 and Figure 84.

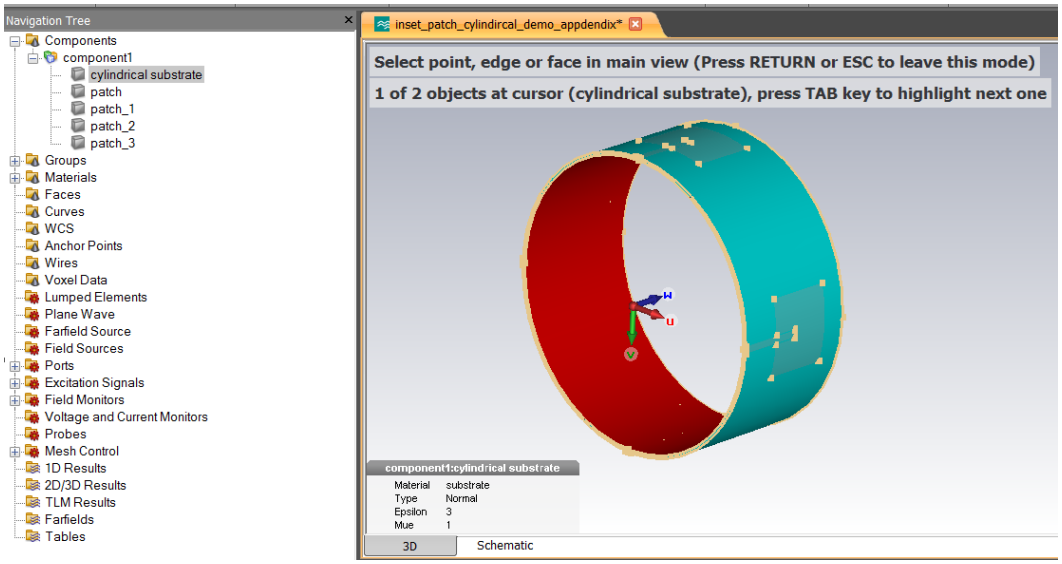

Figure 82 Selection of the inner surface of the substrate

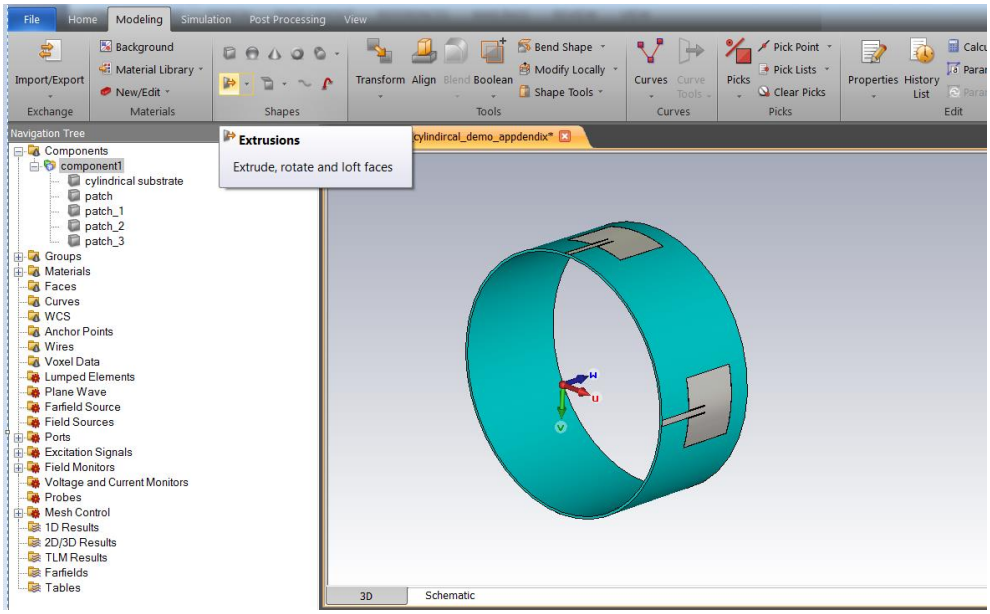

Figure 83 View of the extrusion operation

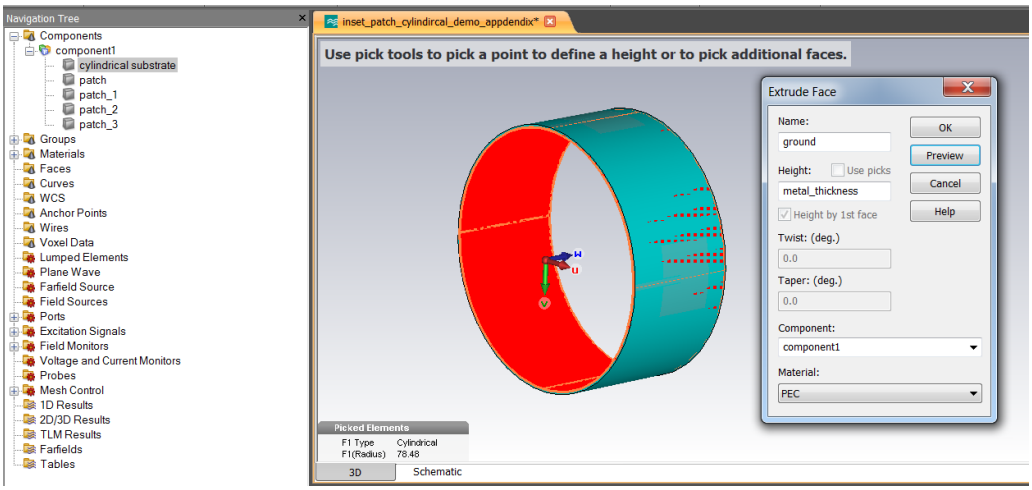

Figure 84 Identifying of the metallic ground plane

After these operations, we can obtain a cylindrical antenna array as given at Figure 85.

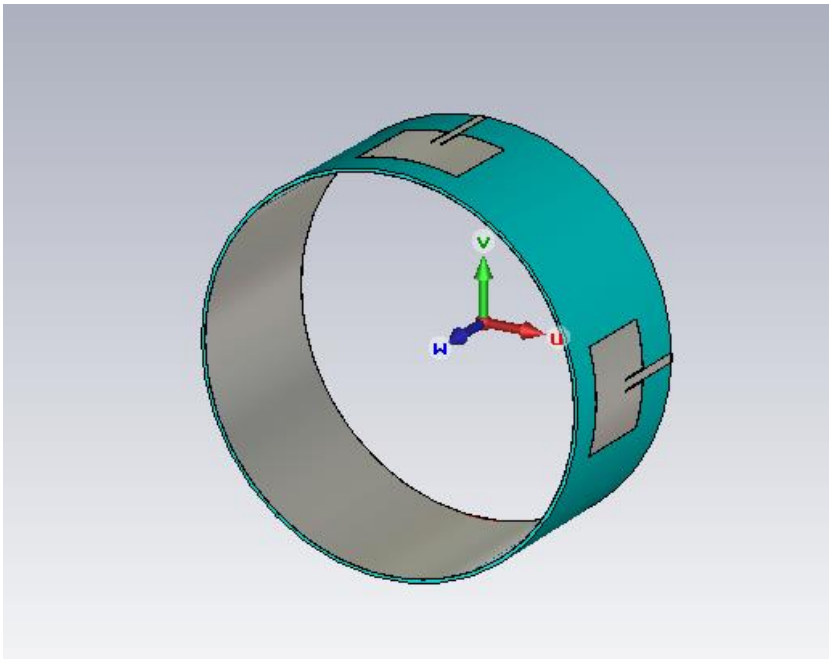

Figure 85 Conformal antenna array